Gas hydrate technology: state of the art and future possibilities for Europe

Technical Report · August 2017

CITATIONS
0

READS
31

26 authors, including:

Peter Gatt
Malta College of Arts, Science & Technology
26 PUBLICATIONS **76** CITATIONS
SEE PROFILE

J. Bialas
Helmholtz Centre for Ocean Research Kiel
161 PUBLICATIONS **1,872** CITATIONS
SEE PROFILE

COST Report

Gas hydrate technology: state of the art and future possibilities for Europe

Contact:

Prof. Dr. Assaf Klar

Phone: +972 4 8292647
E-Mail: klar@technion.ac.il

Prof. Dr.-Ing. Görge Deerberg

Phone: +49 208 8598 1107
E-Mail: goerge.deerberg@umsicht.fraunhofer.de

August 2017

Authors	E-Mail
Prof. Dr. Assaf Klar	klar@technion.ac.il
Prof. Dr.-Ing. Görge Deerberg	goerge.deerberg@umsicht.fraunhofer.de
Dipl.-Ing. Georg Janicki	georg.janicki@umsicht.fraunhofer.de
Prof. Dr. Judith Schicks	judith.schicks(at)gfz-potsdam.de
Prof. Dr. Timothy Minshull	tmin@noc.sotom.ac.uk
Dr. Michael Riedel	mriedel@eps.mcgill.ca
Peer Fietzek	peer.fietzek@km.kongsberg.com
Thomas Mosch	thomas.mosch@km.kongsberg.com
Dr. Umberta Tinivella	utinivella@ogs.trieste.it
Maria De La Fuente Ruiz	mdlf1g15@soton.ac.uk
Dr Peter Gatt	peter.gatt@mcast.edu.mt
Dr. Katrin Schwalenberg	Katrin.Schwalenberg@bgr.de
Dr. Katja Heeschen	katjah@gfz-potsdam.de
Dr. Joerg Bialas	jbialas@geomar.de
Dr. Shmulik Pinkert	pinkert@technion.ac.il
Dr. Anh Minh Tang	anhminh.tang @enpc.fr
Prof. Dr. Bjorn Kvamme	bjorn.kvamme@ift.uib.no
Dr. Erik Spangenberg	erik@gfz-potsdam
Dr. Niall English	niall.english@ucd.ie
Dr. Chazallon Bertrand	Bertrand.CHAZALLON@univ-lille1.fr
Dr. Mahmut Parlaktuna	mahmut@metu.edu.tr
Sourav Kumar Sahoo	sourav.sahoo@soton.ac.uk
Prof. Dr. Klaus Wallmann	kwallmann@geomar.de

Contents

1 Introduction

Interest in natural gas hydrates has been steadily increasing over the last few decades, with the understanding that exploitation of this abundant unconventional source may help meet the ever-increasing energy demand and assist in reduction of CO_2 emission (by replacing coal). Unfortunately, conventional technologies for oil and gas exploitation are not fully appropriate for the specific exploitation of gas hydrate. Consequently, the technology chain, from exploration through production to monitoring, needs to be further developed and adapted to the specific properties and conditions associated with gas hydrates, in order to allow for a commercially and environmentally sound extraction of gas from gas hydrate deposits.

Various academic groups and companies within the European region have been heavily involved in theoretical and applied research of gas hydrate for more than a decade. To demonstrate this, Fig. 1.1 shows a selection of leading European institutes that are actively involved in gas hydrate research. A significant number of these institutes have been strongly involved in recent worldwide exploitation of gas hydrate, which are shown in Fig. 1.2 and summarized in Table 1.1. Despite the state of knowledge, no field trials have been carried out so far in European waters.

MIGRATE (COST action ES1405) aims to pool together expertise of a large number of European research groups and industrial players to advance gas-hydrate related activity with the ultimate goal of preparing the setting for a field production test in European waters.

This MIGRATE report presents an overview of current technologies related to gas hydrate exploration (Chapter 2), production (Chapter 3) and monitoring (Chapter 4), with an emphasis on European activity. This requires covering various activities within different disciplines, all of which contribute to the technology development needed for future cost-effective gas production. The report points out future research and work areas (Chapter 5) that would bridge existing knowledge gaps, through multinational collaboration and interdisciplinary approaches.

Table 1.1: Completed field tests

Year	Location	Description	Duration (h)	Gas production rate (Nm^3/h)	Water production rate (Nm^3/h)	Total gas production (Nm^3)	Total water production (Nm^3)
2002	Mallik 5L-38, Canada	Thermal stimulation	124	4	---	470	---
2007	Mallik 2L-38, Canada	Short pre-test by depressurization	12.5	70	---	830	20
2008	Mallik 2L-38, Canada	Depressurization	144	60-700	0.2-0.6	13000	---
2011	Qilian Mountain, China	Depressurization + thermal stimulation	101	1	---	95	---
2012	Prudhoe Bay, Alaska	CO_2-injection (N_2:CO_2 77:23%) by depressurization	936			24000	180
2013	Nankai Trough, Japan	Offshore field test by depressurization	144	840		120000	1100

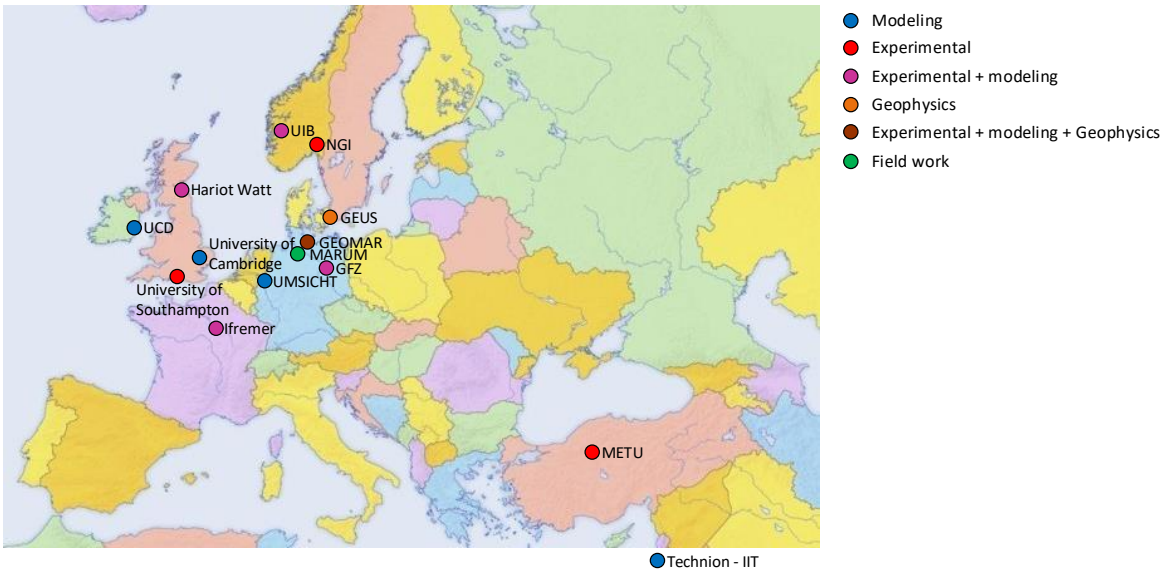

Figure 1.1: Selection of leading European institutes actively involved in gas hydrate research

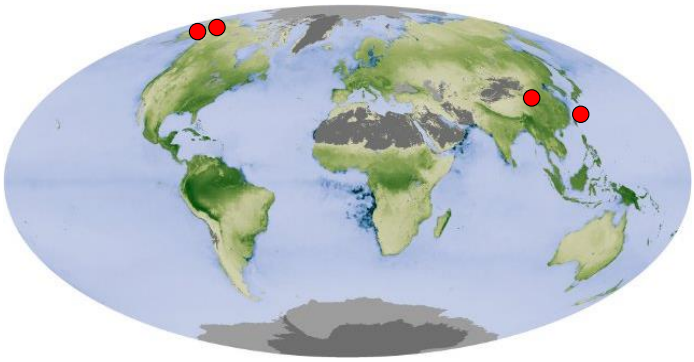

Figure 1.2: Previous production filed test sites

2 Exploration

2.1 Basin Modeling

2.1.1 Petroleum Systems modeling and its premises for modeling gas hydrate scenarios

Gas hydrates are pressure/temperature controlled accumulations of – mostly – methane which occur in sediments at relatively shallow depth. Their existence and (distribution) is of interest for the oil and gas industry due to two main reasons: while gas hydrate accumulations might become a source of energy, they also represent a hazard for drilling and oil/gas transport via pipelines.

Petroleum systems modeling software – typically simulating generation, expulsion, migration, accumulation and hydrocarbon losses in conventional petroleum systems – can also be used to predict

the extent of the gas hydrate stability zone (GHSZ) through geologic time and the formation timing and amounts of gas hydrates within sediments located in the GHSZ.

As petroleum generation is a function of temperature and time, thermal history modeling is a primary goal of petroleum systems modeling. Pore pressure and overpressure modeling is another inherent function required to determine compaction behavior, and therefore widely used for pore pressure predictions. This means that the physical parameters that control the formation and dissociation of gas hydrates are also the most important parameters of modeling conventional petroleum systems.

The process of oil and gas generation from organic matter is commonly represented by chemical kinetic equations, which determine the dependency of the process on temperature and time. As thermogenic gas is often not generated directly, but is obtained from a process of secondary cracking of previously generated oil, secondary cracking kinetics play a critical role for accurate petroleum property predictions. Biogenic gas generation usually occurs at shallower depths and much lower temperatures than thermogenic gas generation. It is commonly simulated by special kinetic reactions available in petroleum systems modeling.

The principle controlling physical rock property for petroleum migration is capillary entry pressure, which offers a resistive force to the movement of petroleum and in effect defines a seal. Different approaches are in use for petroleum migration modeling due to lack of "perfect solutions"; that is, no single method will work for every task and model. The most widely used approaches are Flowpath, Darcy, Invasion Percolation and Hybrid methods.

2.1.2 Characteristics of modeling gas hydrates

The thermal and pressure conditions which control the presence and extent of a gas hydrates stability zone (GHSZ) can change rapidly through geological time. As a result, a GHSZ can be created and then disappear again in cycles of thousands or even hundreds of years. This means that gas hydrate accumulations are also only very short-lived on a geological time scale.

In addition to higher temporal resolution during modeling, higher spatial resolution is also required. The GHSZ is typically up to several hundred meters thick and is independent of the stratigraphy, i.e. of the layer boundaries in a petroleum systems model. High-resolution gridding is therefore required to define the extent of the GHSZ more accurately and to enable gas hydrate accumulations to be meaningfully modeled. The PetroMod simulators have therefore been enhanced (Pinero et al., 2016) to enable minimum cell thicknesses of 10 cm to be used. Beyond that, they offer a minimum time span of 100 years for high resolution modeling in time.

When free gas migrates into the GHSZ, gas hydrates form in the pore space and change the bulk properties of the surrounding lithology. This affects the thermal properties, as the hydrate fills the available pore space with material that has different properties than water. It also affects properties such as porosity and permeability which control the ability of fluids to migrate into the cells. If sufficient amounts of gas are present, hydrate saturations can be high enough to block further flow. These effects can all be assessed with PSM simulators.

2.1.3 Workflow of gas hydrate modeling with PetroMod

The use PetroMod models with gas hydrates modeling is rather straightforward, without special need for changes. If the pressure/temperature (PT) conditions are appropriate, the extent of the GHSZ is calculated through geologic time, and if biogenic and/or thermogenic gas is generated within or migrates into the GHSZ, gas hydrates form and dissociate through geologic time.

The overall workflow can be divided into three main analysis steps:

I. Gas Hydrate Stability Zone (GHSZ) calculation and calibration:

- Set up a standard input model (2D or 3D) and run its simulation in the PetroMod Simulator;
- Display and analyze results (e.g. existence and dynamic of the GHSZ) in PetroMod Viewer;
- Check calibration match with known data, if available.

II. Gas Hydrate formation calculation and calibration;

- Adjust the resolution of the models grid to match the spatial dynamic of the GHSZ;
- Adjust the temporal resolution of the model to match the dynamic of the GHSZ through time;
- For (onshore) models in arctic climate regions define permafrost limits;
- Enable formation of gas hydrate in specific lithologies and adjust values for salinity (open water as well as porewater) and a grid-cells minimum gas saturation if necessary;
- Select additional overlays and select the migration method;
- Re-run the simulation;
- Check calibration with known data if available.

III. Model refinement

- Adjust the PVT conditions of gas hydrate formation and gas hydrate parameters via PetroMod editors;
- Add special kinetic reactions to mimic a biogenic generation of gas via the PetroMod editors.

2.1.4 Analyzing a petroleum systems model showing gas hydrate accumulations

A resulting model - either in 2D or in 3D - can show the existence of the GHSZ and its evolution in space and time. In case of an existing GHSZ, the formation of gas hydrate accumulations can be shown through time as well as the decay of these accumulations if PT conditions change. Because PetroMod can track the generation, migration and accumulation of single hydrocarbon components, it is also possible to follow the pathways of a hydrocarbon component of interest through space and time.

Fig. 2.1 shows a PetroMod 3D model located within the Alaska North Slope. Therein conventional as well as gas hydrate accumulations can be observed. Furthermore, it is shown that a biogenic methane fills up the gas hydrate accumulations while the conventional accumulations are dominated by thermogenic methane.

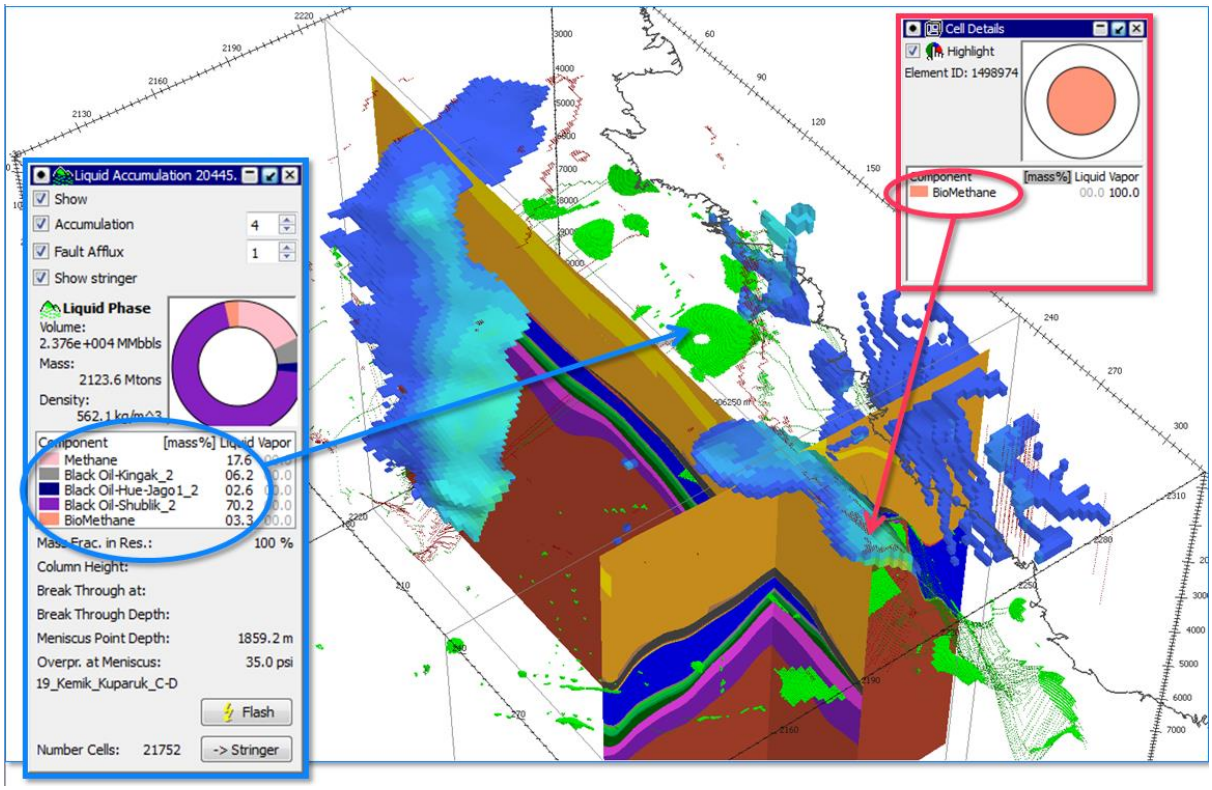

Figure 2.1: Alaska North Slope 3D petroleum systems model showing gas hydrate accumulations (blue) in the GHSZ, conventional accumulations (green) and tracked biogenically vs. thermogenically sourced methane.

2.1.5 The possible future of gas hydrate modeling

To increase the quality of modeling gas hydrate scenarios, some improvements of modeling software are necessary. Further increasing the possible resolution in time and space would result in a more detailed view and outlook of the evolution of gas hydrate accumulations.

An option to display BSR(s) as surface(s) within simulated scenarios would improve the understanding of gas hydrate scenarios in general by displaying multiple BSRs. Last, but not least, it is of vital interest to treat gas hydrates as a physical phase on its own to better distinguish them from the liquid and vapor phases of conventional petroleum systems modeling.

2.2 Geophysics

Usually gas hydrate reservoirs are found at continental slopes where seafloor dips towards the abyssal plains (Kvenvolden, 1993; Wallmann et al., 2012). Natural gas expulsion points towards larger accumulations of free gas as a first hint for possible hydrate reservoirs (Judd and Hovland, 2007). Water column imaging capabilities developed for multibeam acquisition systems nowadays allow a rapid mapping of prospective areas (Schneider von Deimling and Papenberg, 2012). However production of hydrate reservoirs (Wallmann and Bialas, 2009) need to be well separated from natural leakage systems to avoid uncontrolled elusion of gas. A reasonable sealing overburden need to be confirmed to protect against formation of artificial leakage out of the reservoir once hydrate dissolution has been

stimulated. With respect to optimal production rates of dissolved methane porosity of hydrate bearing layers is another issue. Therefore, coarse grained sandy reservoir rocks overlain by clay provide the best environment. Due to the unconsolidated sediment matrix of the host rock, slope stability is an issue in terms of seafloor installations and possible deepening of the seafloor above the production site (Zander et al., 2017).

Geophysical investigations provide a key technology aiming for lateral imaging of dedicated gas hydrate reservoirs, distribution of free gas and related migration pathways. Thereby geophysical techniques try to make use of the anomalous physical properties related to emplacement of gas hydrates (increased sound velocities, increased density, modified elastic modulus, increased resistivity) and free gas (reduced sound velocity, reduced density, modified elastic modulus, increased resistivity) compared to the unaltered matrix sediment. The most sensible tools available for the remote and areal observation of these physical parameters are seismic and controlled source electromagnetic measurements.

2.2.1 Seismic methods

A first identifier for gas hydrate occurrence is the bottom-simulating reflector (BSR) (Kvenvolden, 1988; MacKay et al., 1994). The BSR is caused by the negative impedance contrast caused by free gas accumulated underneath the gas hydrate seal above (MacKay et al., 1994). Thereby the BSR documents the lower boundary of the gas hydrate stability zone (GHSZ). These events are visible in standard exploration configurations with low source frequencies (e.g. large airgun arrays, up to about 100 Hz) and standard multichannel streamer (MCS) configurations (min. 12.5 m group offset). However improved resolutions like vertical seismic profiles (VSP, onshore examples) show lateral variations in reflection strength and continuity of the BSR (Bellefleur et al., 2006). Due to increased source frequencies (up to about 350 Hz) and increased streamer resolution (group offset of 1.5 m) such effects become visible in marine data as well. Focusing on the production of gas hydrates the plumbing system of methane is of high importance. Not only the provision of free gas for the hydrate formation but also natural gas migration pathways are important to judge on the tightness of the desired reservoir (Koch et al., 2016; Krabbenhoeft et al., 2013). 3D high resolution seismic imaging tools like the recent P-Cable development are capable to provide migrated sub-bottom images down to 6 m by 6 m gridded volumes (Bialas, 2013; Bialas and Brückmann, 2009; Petersen et al., 2010). Such volume observations are required to estimate hydrate distribution and hence available volumes as well as to investigate vertical migration pathways through the GHSZ. Due to their gas content, such chimneys are described as blanking zones on seismic sections. They may link the BSR to active gas expulsion sites at the seafloor bypassing free gas through the hydrate stability field (Hustoft et al., 2009; Judd and Hovland, 2007; Klaucke et al., 2015; Koch et al., 2016; Talukder, 2012). They may occur at the top termination of open fractures now originating within the GHSZ and they may be terminated by inverted reflection events well beyond the seafloor when the gas transport got stuck for various reasons (Koch et al., 2016; Plaza-Faverola et al., 2014). During gas production chimneys could result into uncontrolled gas emissions and need to be avoided. As the vertical orientation might not be straight, 3D images are required in order to not lose track of such structures when investigating a possible production site.

Another approach in 2D seismic investigations is the application of deep towed multichannel streamers. The idea is to increase resolution by reducing the offset between receiver and target (Breitzke and Bialas, 2003; Talukder et al., 2007) or both source with receiver and target (Gettrust et al., 2004; Marsset et al., 2014). Thereby reducing the Fresnel Zone the lateral resolution is increased. In addition hybrid systems using surface towed sources and deep towed multichannel streamers provide wide-angle reflection surveys, which enable to undershoot strong reflecting near surface structures (Breitzke and Bialas, 2003). This ability allows to image vertical migration pathways underneath possible gas accumulations in their chimney top. Combined systems of deep towed source and receiver on the other hand allow the use of higher frequent sources (Marsset et al., 2014), which usually provide lower energy than standard airgun sources. However, due to the reduced offset penetration it is good enough to image gas hydrate relevant structures with increased vertical resolution.

Besides reflection seismic characterization, sound velocity anomalies are a second criterion to judge on free gas and hydrate distribution in the sediment. While short active length multi-channel reflection seismic streamers (in 2D and 3D) are already capable to provide the required images, by use of mid size multi purpose vessels they are usually not sensible enough to velocity. This gap can be closed by use of ocean-bottom seismometers (OBS) (Crutchley et al., 2016; Petersen et al., 2007). Equipped with 4 component receivers they provide wide reflection and refraction observations not only for compressional waves (V_p) but for converted shear waves (V_s) as well (Bialas et al., 2017; Granli et al., 1999; Lee and Collett, 1999). Usually deployments of OBS take place together with 2D and 3D profiling above gas hydrate reservoirs. Depending on water depth and lateral offsets refraction events are usually expected for layers beyond the BSR and the interpretation of OBS events will concentrate on wide angle reflections. Correlations of OBS and MCS data enables safe identification of major interfaces and guides the definition of a starting model for the velocity-depth distribution used to invert for the observed travel times. Velocity anomalies coincident with increased reflection amplitudes provide first hints for possible hydrate or gas accumulations. Further information on physical parameters are available when converted shear wave events are provided by seismometer records. Different dependency on elastic moduli allow to further discretize on free gas and hydrate distribution (Yun et al., 2005). Increasing precision on navigation, dense shot coverage and observation of 3D airgun signal generation allow for 3D inversion of OBS data, supporting the volume analyses of velocity anomalies and implied gas and hydrate distributions. Modern parallel node computing clusters allow employment of new processing technologies like full-wave form inversion (Pecher et al., 1996; Virieux and Operto, 2009) for OBS data as well. Hereby ray tracing based velocity models are required as detailed starting models in order to further improve the velocity depth resolution.

2.2.2 2D & 3D high resolution reflection seismic imaging (P-Cable)

A new high-resolution multichannel reflection seismic tool has been provided by the invention of the so called P-Cable (Plancke and Berndt, 2002) acquisition system. The P-Cable allows for three-dimensional seismic imaging of the shallow horizons with increased resolution (6 m by 6 m) operating from a non-specialized vessel with small crew.

Compared to standard reflection seismic applications in 2-D and 3-D the basic difference is that the P-Cable is built by a cross cable towed perpendicular to the ships heading (Fig. 2.2). Instead of a few single streamers the P-Cable uses a large number of short streamer sections towed parallel from the cross cable. Drawback is the limited depth penetration due to the short offsets, which limits removal of multiple energy. This is well compensated by the reduced costs of the system and the ability to operate it even from small multi purpose vessels, the usual academic platform for marine research.

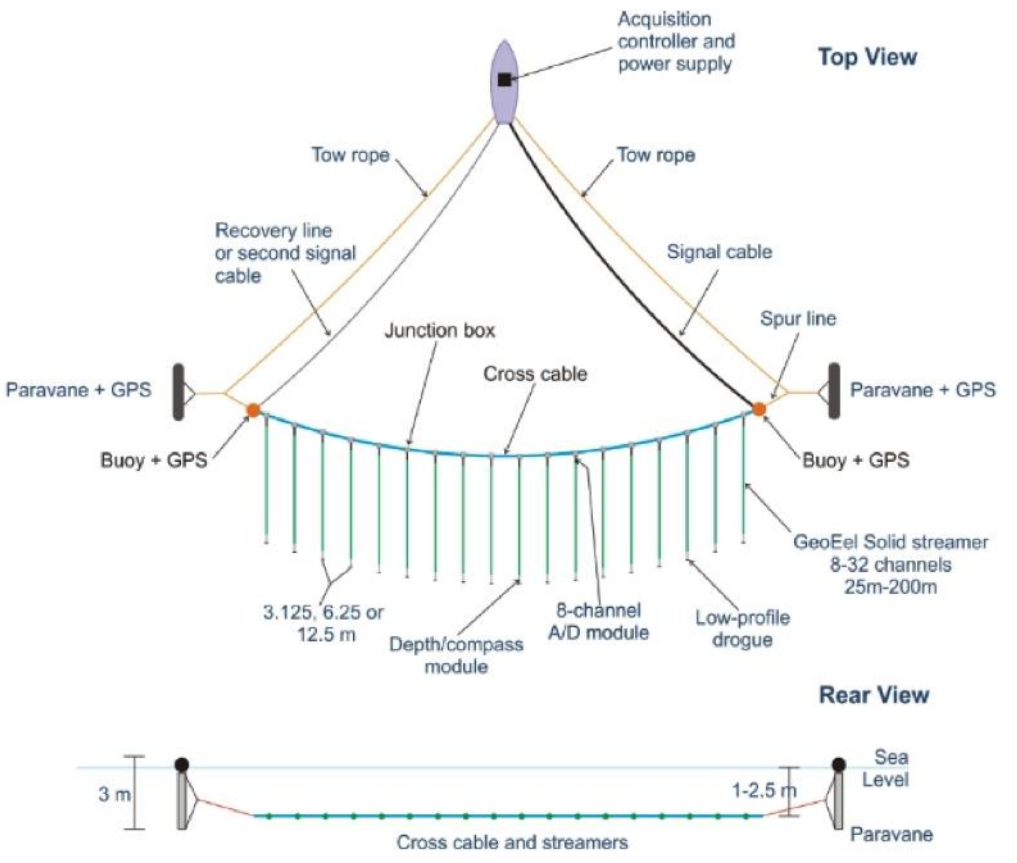

Figure 2.2: Schematic drawing of a P-Cable deployment. Descriptions in the figure identify the best grade of configuration in terms of navigation aids and hence resulting resolution. However minimum request are GPS recordings from the paravanes in order to calculate the cross cable layout. (courtesy of GEOMETRICS, USA).

Positions of the trawl doors with real coordinates and relative distance to the vessel are provided within an online navigation package. Autonomous GPS receivers were mounted on each trawl door together with a serial radio link to the vessel. Depending on the grade of configuration compass and/or depth readings at each streamer breakout point maybe provided as well. Based on these information navigation processing attempts to best calculated the layout of the cross cable and adjacent streamer

sections for each shot. In general, a catenary geometry fits the curvature of the cross cable best. Standard filter and deconvolution routines prepare the data volume for a 3D migration.

Resulting seismic sections from the 3D data volume provide a much more detailed image of subsurface structures like gas chimneys and sedimentary interfaces than conventional data do (Fig. 2.3 (Petersen et al., 2010)). Such resolutions are required to map out BSR distribution and continuity in the hydrate stability field. Knowledge of gas migration pathways is a prerequisite in description and safety assessment of a possible GH reservoir in order to avoid uncontrolled gas emissions during production. No other system can provide such information with reasonable resolution. However, one drawback is the missing sensibility of the short offset streamer segments to the velocity field in the subsurface. Stacking and migration of the data need to be done for near vertical reflection points only and hence can be completed with water sound velocities. Observation of the seismic signals by a suitable number of Ocean-Bottom Hydrophones (OBH) or four component Seismometers (OBS) can provide this information.

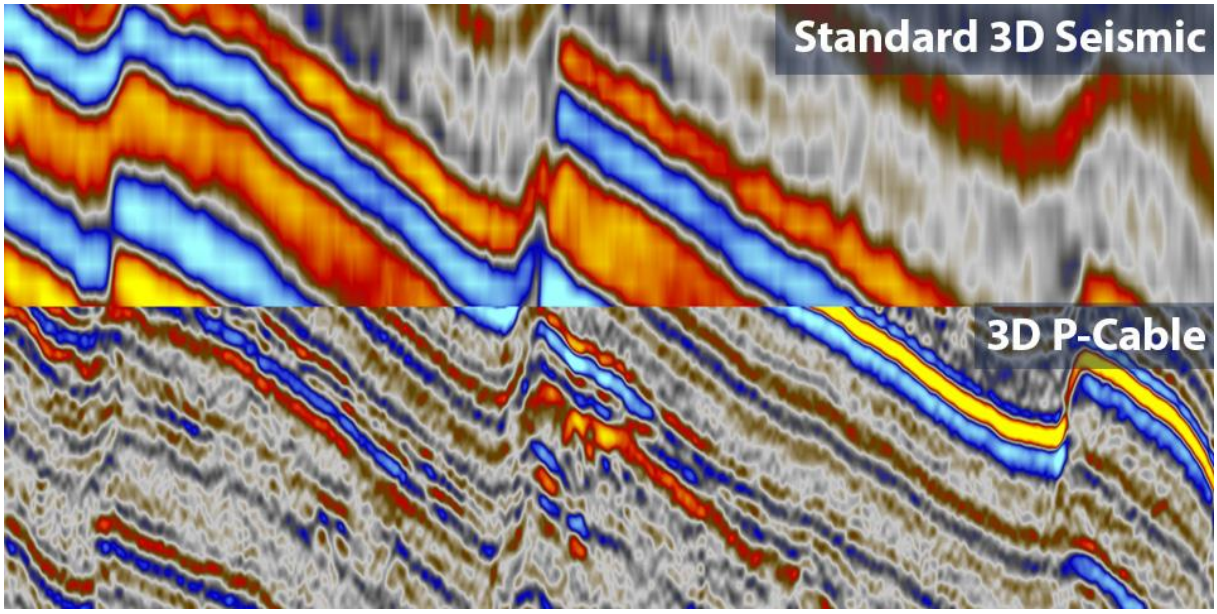

Figure 2.3: Comparison of standard 3D seismic and 3D P-Cable data from overlapping records (courtesy WPG exploration Ltd., http://www.wgp-group.com; *p*-Cable Spring Energy report)

2.2.3 High resolution refraction seismic imaging (OBS)

Besides reflection seismic events (increased amplitudes, inverted amplitudes, BSR, etc.) seismic velocity anomalies (*p*- and *s*-wave) and corresponding Poisson's ratios may further support identification of gas or hydrate distribution (Tinivella and Accaino, 2000). Simultaneous recording of multichannel and ocean-bottom seismometer data allows correlation of events from reflection seismic images with near vertical reflection events from OBS records (Fig. 2.4). Thereby travel-time picks taken from the OBS records for velocity depth model development can be chosen to fit to the major sedimentation packages already. Overlay of the resulting velocity – depth model with multichannel

seismic sections will further support the interpretation of hydrate and free gas distribution in a reservoir environment. Besides standard ray tracing and tomographic inversion routines full-waveform inversion (Virieux and Operto, 2009) has been extended to refraction seismic applications and supports more detailed inversion models in future time.

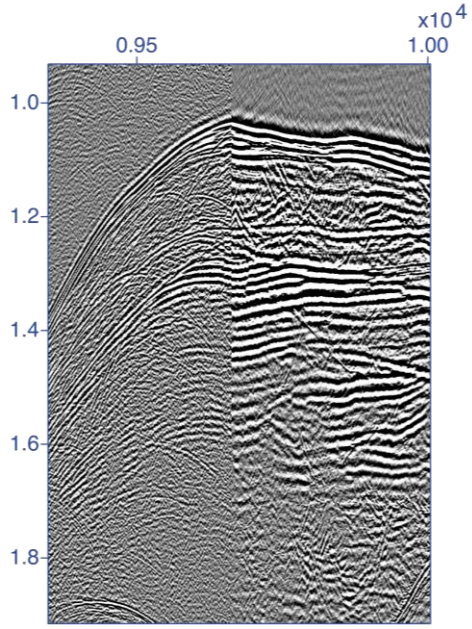

Figure 2.4: Correlation of near vertical reflection events recorded by an Ocean-Bottom Seismometer (OBS,; left hand) and the corresponding multichannel seismic section.

Based on significant impedance contrasts across sediment interfaces compressional waver energy converts partly into shear wave components, which were recorded by horizontal receivers of the seismometer components of the OBS. Due to the unknown orientation of the seismometer all three components need to be evaluated for their amount of shear wave energy, which results in energy rotation processing prior to analyses of the radial horizontal component (Wang et al., 2014). For the interpretation a *p* to *s* conversion is assumed to happen at the reflecting sediment interface (Zillmer et al., 2005). Other assumptions could solve the observed travel-times but require unreasonable low velocities. Due to the high attenuation of shear waves in unconsolidated sediments high V_p/V_s ratios are indicative for the expected low shear wave velocities. Consequently, angles of refraction and reflection are small compared to *p*-wave expansions and therefore the portion of sub-surfaces structures imaged by converted shear waves are smaller than by *p*-waves (Fig. 2.5). Usually the sensor distribution is optimized for *p*-wave recordings resulting in gaps of *s*-wave coverage. As a result, V_s model development for the entire profile results in significant smoothing. Detailed analyses and interpretation of conventional shear wave data either request optimized (shorter offset) sensor distribution or localized analyses (Fig. 2.5).

Based on velocity anomalies first estimates on hydrate and free gas distributions along the BSR and within the hydrate stability zone are undertaken. Without additional information such estimates can be of qualitative value only as a deduction of hydrate saturations strongly depend on the formation process. In case of sediment matrix supporting hydrate formation the elastic moduli and hence V_p and

V_s are much stronger influenced than with hydrate grains in the pore space (Chaouachi et al., 2015; Priest et al., 2009). Making use of their different relation to physical parameters correlation of seismic velocity models with electromagnetic investigations (CSEM) provide additional information. Coupling seismic and CSEM investigations by transverse functions for their model space enables joint inversion with much more detailed information about physical parameters (Heincke et al., 2017) in future time.

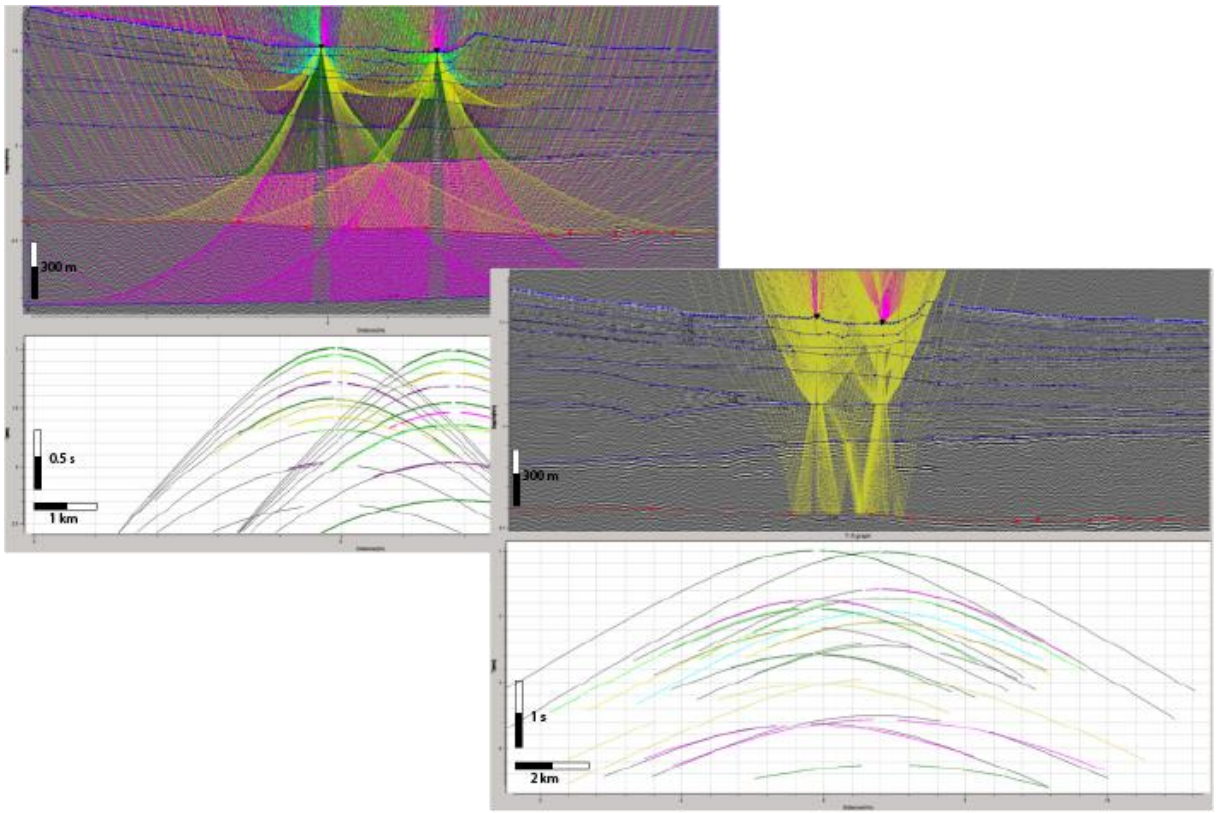

Figure 2.5: Examples of V_p (upper left) and V_s (lower right) ray coverage of subsurface structures. Ray paths used for the inversion of OBS data are overlain on reflection seismic images used to identify the relevant sediment interfaces. Due to the low shear wave velocity reflected converted waves can image smaller parts of the model space only. However they can contribute to detailed investigations of velocity anomalies and hence physical parameters. Picked (black) and computed (colored) travel-times are displayed beyond the seismic sections (Bialas et al., 2017).

2.2.4 Marine CSEM Methods

Additional information on hydrate and gas distributions are provided by application of marine controlled source electromagnetic (CSEM) methods (Attias et al., 2016; Hölz et al., 2015). Electrical resistivity derived from CSEM data is sensitive to porosity and the electrical properties of the pore fluid. As free gas and gas hydrate are electrically resistive, the replacement of saline and therefore conductive pore fluids by resistive gas and / or gas hydrate increases the formation bulk resistivity. Discrimination between free gas and gas hydrate from electrical resistivity requires additional information from e.g. seismic and knowledge of the geological setting. Within the gas hydrate stability

zone, free gas will be consumed by gas hydrate formation as long as the gas content exceeds the solubility of gas and sufficient water is supplied. According to Liu and Fleming (2007) free gas and gas hydrate may coexist within the GHSZ when *i*) the gas flow and gas pressure from below the GHSZ is accordingly high, often indicated by sub-vertical chimney structures in reflection seismic images. *ii*) when all water is depleted due to concentrated hydrate formation, or *iii*) upward perturbation of the *P-T* boundary caused by advecting warm fluids.

Small gas and gas hydrate saturations (saturation defined as percentage of pore volume opposing to concentration defined as percentage of sediment volume) in the order of a few percent may scatter and blank out reflection seismic signals. In contrast, large volumes of gas and gas hydrate in the order of >10-20 % are required to significantly increase the bulk resistivity derived from CSEM leaving smaller saturations subject to possible misinterpretation due to lithology-controlled porosity changes.

Electromagnetic field propagation is a diffusive process. Thus, CSEM measurements provide volume information useful for resource assessment and lack detailed structural resolution. This promotes the combination of seismic and CSEM methods, as they are complementary with respect to their information content.

Marine CSEM Instrumentation

Both time domain and frequency domain CSEM systems have been developed using either magnetic or electric source and receiving dipoles close or on the seafloor. The first marine CSEM experiments for the exploration of submarine gas hydrates have been conducted with a time domain, seafloor-towed, electric dipole-dipole systems developed at the University of Toronto (Edwards, 1997) measuring the inline component of the electric fields at offsets of up to 600m sensitive to sediment depth of ~200-300m. First case studies have been reported by Yuan and Edwards (2000) and Schwalenberg et al. (2005, 2010a, 2010b). An advancement of the Toronto system is the HYDRA system developed at the Federal Institute for Geosciences and Natural Resources (BGR). HYDRA is a modular, seafloor-towed electric dipole-dipole system with four or more receiver dipoles at offsets up to 1000m. It has been recently updated to allow online communication and data transfer during deployments. Data have been collected over gas hydrate targets offshore New Zealand (Schwalenberg et al., 2017) and in the Black Sea (Schwalenberg et al., 2016).

A smaller seafloor-towed magnetic dipole-dipole system with short offsets up to 40m has been developed at the Woods Hole Oceanic Institute (WHOI), and has been used at a gas hydrate mound in the Gulf of Mexico (Ellis at al., 2008).

The advantages of the seafloor-towed systems are that they can be operated with a small team, surveys can be adapted to smaller scale targets, navigation errors are minimized, and data analysis is straight forward. The disadvantages are the risk of damage to or loss of the system or parts of it, thus surveys are limited to rather smooth sediment (which is typically the case along continental slope areas).

The nowadays most commonly used marine CSEM approach for gas hydrate research has been pioneered by Scripps Institution of Oceanography, and is an adaptation of the experimental setup used in the offshore oil and gas industry (Constable, 2010). This setup includes a number of stationary seafloor ocean bottom electromagnetic (OBEM) receivers deployed from the vessel along a survey line

or on a 3D grid, and a CSEM transmitter with a horizontal electrical source dipole, typically 50-200m long, towed by the research vessel about 50 to 100m above the seafloor. Frequency domain data are collected using a modulated wave form (e.g. Myer et al., 2010), and inverted to 2D and 3D resistivity models using various transmitter-receiver offsets corresponding to different penetration depth. Gas hydrate case studies using this setup have been published by e.g. Weitemeyer et al., (2006, 2010, 2011), Goswami et al., (2015), and Attias et al., (2016). The advantage of this setup is that large areas can be covered and penetration depth can be more than 1000 to 2000m below seafloor. Also inline and broadside data can be collected using both orientations of the OBEM receiver dipoles. The disadvantage is that navigation errors can be severe, particularly at smaller offsets, and small-scale features, i.e. local gas hydrate accumulations, may be overseen.

An advancement is the Vulcan system developed at Scripps (Constable et al., 2016) consisting of one or more three-axial electric dipole receivers towed in the water at offsets of some hundred meters behind the source dipole. This setup allows a quick survey progress and penetration depths down to ~1000m of sediments. Gas hydrate case studies have been reported in Weitemeyer et al. (2010), Goswami et al., (2015), Attias et al., (2016), Constable et al. (2016).

A rather unique CSEM setup for gas hydrate exploration has been developed at GEOMAR using stationary seafloor electromagnetic (OBEM) receivers deployed on a 2D line or 3D grid at short offsets, and a mobile CSEM source called Sputnik with two 10m long horizontal source dipoles. Sputnik is powered and communicates via the deep tow cable which is used to move it along the seafloor by lifting up and down the deep-tow cable. The advantage of this setup is a detailed and small-scale 2D or 3D data set focusing of target areas of particular interest. The disadvantage is the navigation, i.e. transmitter receiver offsets and orientations must be known accurately.

In summary, various CSEM experimental setups exist capable to focus on different aspects of the gas hydrate stability field. CSEM data analysis and interpretation has been significantly improved since 2D inversion tools (e.g. Key et al., 2016) and 3D forward modeling codes have become available. Joint interpretation of marine CSEM and seismic data highly improves the conclusions on gas hydrate resource assessments. While density is a joint physical parameter in the equations solving model calculations for seismic velocity and CSEM data joint inversion of these data sets data is a key to further constrain resource assessments (Abubakar et al., 2012; Hu et al., 2009).

Laboratory experiments on hydrate formation models further guide how to translate velocity anomalies into hydrate and gas concentrations. As relations of velocity and concentration are significantly different depending on the relevant hydrate formation model (pore filling, matrix supporting) in situ calibration information is necessary (Jing and Xuewei, 2011; Lee and Collett, 1999).

2.3 Drilling

The drilling process itself is only a part of the final construction of a wellbore. The long-term use of the wellbore and its safe operation require pipes which are introduced and cemented within the sediment formation. The structure of the well must withstand the pressure difference between the wellbore

(e. g. hydrostatic and drilling fluid pressure) and formation (formation pressure) which develops throughout the exploitation process. Along the wellbore path, both horizons with overpressure (potential fluid inflows from formation) and horizons with underpressure (drilling fluid losses to the formation) may exist and must be managed specifically to adapt the drilling parameters accordingly. The drilling of the well should therefore be planned in accordance with the anticipated conditions. Common state-of-the-art drilling methods from the oil and gas industry are (*i*) *rotary drilling*, (*ii*) *coiled tubing drilling (CTD)*, (*iii*) *jetting* and (*iv*) *casing drilling*. All of these drilling methods may be used for drilling a vertical well or in case of directional drilling. This document extends briefly on the first two methods.

The *rotary drilling* method is characterized by a rotating drill string and a circulating drilling fluid (liquid and gaseous and mixtures of fluids and solids). The drill string connects between the drilling tool at the downhole and the drilling rig at the surface. Typically, it consists of individual drill pipes and is, therefore, also called *jointed pipe*. A very simple drill string for a vertical well consists of (from the bottom up): drill bit, drill collars (DC), heavy weight drill pipes (HWDP) and drill pipe (DP). The drill pipe is connected to the rotary drive/drill floor of the drilling rig at the surface. The standard length of a drill string component is about 10 m (33 feet). A continuous circular motion of the drilling bit (fixed cutter, roller cone or hammer bits) causes breakage of the formation (cuttings) at the bottom of the borehole. In a closed circuit, (fresh) drilling fluid is pumped down (inside) the drill pipe to the bit where it removes the cuttings from the borehole and carries them through the annular space between the pipe and borehole wall to the surface. Drilling fluid on the surface is processed and injected back into the drill pipe. Recycling, treatment and conditioning of drilling fluids are appropriate measures to minimize operational costs.

In contrast to standard rotary drilling with jointed pipes, during *coiled tubing drilling (CTD)* no assembling of individual drill pipe components is necessary. Therefore, once started, the drilling fluid flow cannot be interrupted. Thus, the CTD method is significantly faster than rotary drilling (two to three times) and reduces the running costs compared to the jointed pipe method. As the drill string of a CTD cannot be rotated, a bottom hole assembly (BHA) must be attached to control the drill head. In many cases, the BHA is similar to that for jointed pipe and consists of (from the bottom up): drill bit, drill motor (with orienting tool), usually MWD (measurement-while-drilling) and LWD (logging-while-drilling) devices (see below) and stabilizers. Drill collars or HWDPs can only be installed directly above the BHA. Therefore, it is difficult with directional drilling to apply pressure on the drill bit. The removal of cuttings through the annulus may be hampered by the lack of rotation especially in deflected wellbores, so that the tubing sections may get stuck. CT drill strings have substantially smaller diameter than jointed pipes. CTD is also ideal for underbalanced drilling as the drill string is a closed system and, therefore, produced reservoir fluids cannot escape to the string. A CT-well can only be as long as the tubing itself. The length of the tubing sections of the coil depends on the diameter. Thinner tubing decreases the horizontal drilling distance.

In general, wellbores are planned and completed according to the geological profile assuming a certain depth and diameter of the final casing. The geological profile is used to identify problematic horizons (aquifers, formations with overpressure or underpressure, unstable horizons etc.) that need to be isolated resulting in a specific well construction (Fig. 2.6). Normally, it consists of standpipe, conductor pipe, functional pipe strings as needed and production casing string.

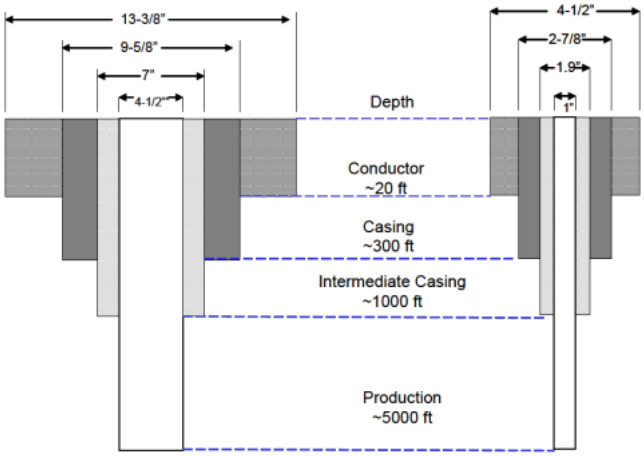

Figure 2.6: Illustration of a vertical wellbore completion. Conventional (left) and CTD (right) (Perry et al., 2006).

In the well construction process, the selected pipe strings are cemented in the sediment one after the other, leading to a "tight" structure. Individual cement layers must overlap. The outer diameter of the string and the drill bit diameter are standardized by the API (American Petroleum Institute). While the initial diameter of the wellbore depends on the geology, the final depth and diameter are determined by the expected production rate and the specific application. For example, exploration wells are completed with special measuring devices at the depth of the deposit to be explored. Therefore, they usually have relatively large diameters. Oil and gas wells often have end diameters of 6 or 8½ inches. Smaller diameters (e.g. 4") are mostly used for re-entry drilling (sidetrack). In addition, so called slim-hole or micro-hole wellbores with diameters of ~1 to 3 inches exist and have already been realized with CTD to a depth which is usually sufficient for the exploration of gas hydrate.

In the past, directional drilling became a state-of-the-art method to control a wellbore trajectory, to drill complex geological structures and to make previously unreachable reservoirs accessible. The directional drilling includes a controlled drilling to follow a desired wellbore pathway. This can be implemented differently, e.g. with steerable drill motors (Push-the-Bit, Point-the-Bit) or by mechanical devices within the drill string (whipstock). Due to the high costs of a deep well, new techniques are being developed to increase the productivity of a single wellbore. Fig. 2.7 shows possible well profiles (short, medium, long). However, drilling very small radii is restricted because of the limited ability to withstand the high forces (flexural and frictional) that develop. Very sensitive sensors may detect minimal deviations from the planned pathway and are adjustable to maintain the planned wellbore trajectory very accurately. In general, one may say that a larger well diameter increases the radius of a directional well.

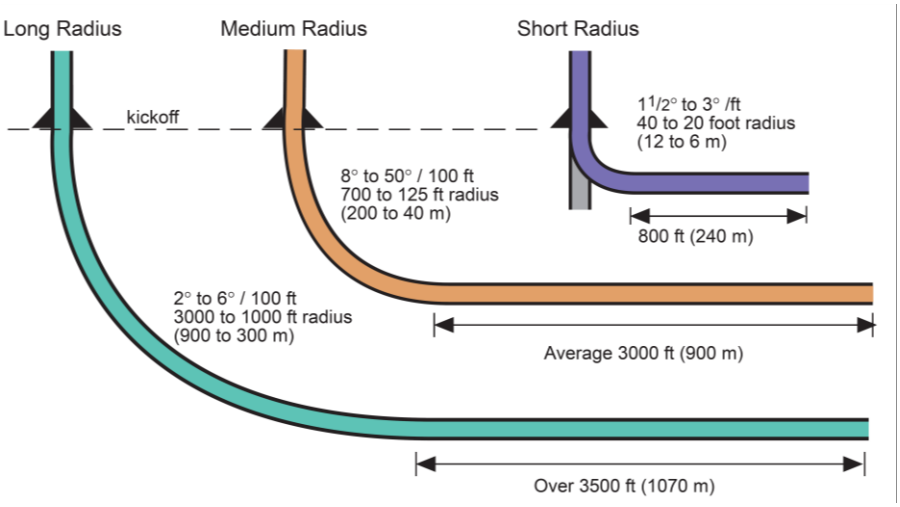

Figure 2.7: Schematic diagram of directional drillings (Jahn et al., 2008, Hydrocarbon exploration and production).

Drilling through, and into, a gas hydrate formations entails special requirements on the drilling fluids and the sealing between the well and the formation. If directional drilling is the only feasible economic alternative, the formation structure has to be stable in both the drilling stage and later at the production phase. Currently, there is a lack of corresponding geological and geophysical evaluations. Moreover, simulations of the mechanical stressing of gas-hydrate horizontal wells infer that the stressing mechanism may be significantly different from that of conventional horizontal wells (e.g. Klar et al., 2010).

In some cases, where the geomechanical properties of a gas hydrate deposit allow, the application of hydraulic stimulation might be considered. The effect of this would be to effectively create extra permeability around the existing wellbore allowing access to a greater volume of hydrate-rick sediment and also allowing faster production of released gas.

The navigation of the drill bit requires the availability of numerous measurement techniques and high-tech instruments. Among others, MWD and LWD are common. Usually, modern downhole instruments are optimized combinations of MWD and LWD devices, and include additional sensors for temperature, pressure and vibration, and others for data measurement allowing fast and safe drilling. In addition to *indirect* methods, in-situ measurements during the drilling phase can give immediate information about geological properties of the sediment. Thus, required data for gas hydrates in the sediment can be collected. LWD and MWD are both tools that are installed within the drill string and take measurements at each survey. In contrast to MWD, which determines the position of the wellbore (geometrical navigation), LWD measures formation properties (formation evaluation). LWD allows an exact identification of the deposit, even if its position has been known only roughly before the beginning of drilling (e.g. from seismic surveys and exploration drilling). LWD also enables navigation within the deposit based on reservoir properties (geosteering). Geosteering, with horizontal well, is a state-of-the-art tool for the exploitation of thin deposit layers. Moreover, natural gamma ray, resistivity log as well as measuring devices with radioactive sources (gamma ray, neutron porosity tool) are standard tools for deep drilling. Due to the high safety requirements for using radioactive sources they are, however, only used when absolutely necessary. Other available equipment on the market

are the NMR (nuclear magnetic resonance), Sonic logs or Acoustic Well Log and formation tester and sampler as well as radar navigation and data transmission for control of the drill bit (for directional drilling). All of these methods are also suitable for detection of gas hydrates in sediments, and provide reliable results. Development of, modern technology will facilitate access to gas hydrate layers of several meters in shallow depths, either. In summary, one may say that a combination of several measuring method is crucial for a safe identification of gas hydrate layers. The required instruments are state-of-the-art and already available on the market for common wellbore diameters (~ 5''). Possibly, special equipment must be built for slim-hole or short radius applications.

Since the drilling is one of the major cost factors in the production of natural gas and, in particular, from gas hydrates, new lightweight and very flexible subsea rigs need to be developed. Supposedly, none of the gas hydrate deposits will provide high coherent gas reserves, and low production rates can be expected only on a temporary basis. Consequently, appropriate considerations for effective drilling techniques need to be made, and Europe has at least two such systems:

1) The *MeBo200,* developed by Bauer Maschinen GmbH and MARUM (Figure 2.8), may be valuable tool of an effective solution scheme.

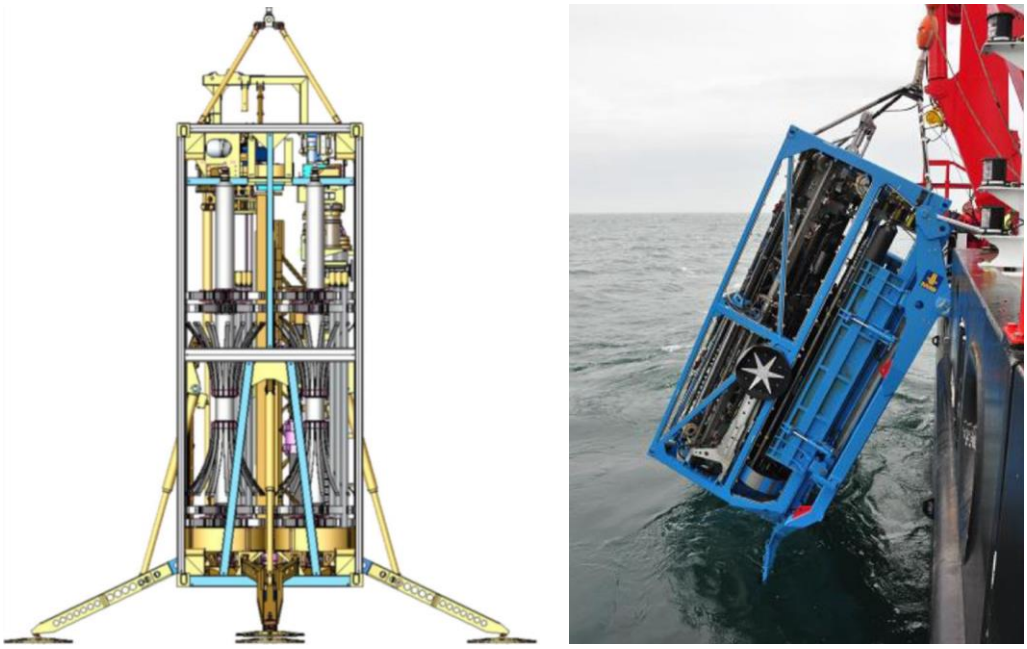

Figure 2.8: Sketch of the MeBo200 developed by MARUM and BAUER Maschinen GmbH (left) and deployment of the MeBo200 (right) (Spagnoli et al., 2015).

In order to avoid the time-consuming assembly of a drill string from the drillship to the seafloor, it is preferable to use drill rigs placed on the seafloor, which safe time and costs. The MeBo200 drilling rig will may be lowered to the seafloor and operate remotely from the ship, drilling up to 200m into the seafloor. The MeBo200 does not require a special drill ship, as the rig itself has the size of a 20 ft container. It is equipped with a rotary drill head and a carousel storage and handling system for drill rods. The drill rods are taken from the carousel and inserted successively into the drill string. Thus, the wellbore can be drilled in several sections directly from the seafloor, and, consequently, the drilling process becomes more cost-effective

and independent from bad weather conditions (wind, currents, and waves). The MeBo200 has already been used successfully for coring sediments containing gas hydrates. (Spagnoli et al., 2015).

2) The BGS Rockdrill (RD2), seen in Fig. 2.9, is capable of coring up to 55m below sea floor in water depths up to 4000m and is operated via its own launch and recovery system (LARS). The system can continuously core in 1.7m sections, and can be outfitted with additional sensors such as gas-flow meters and down-hole logging tools. RD2 has been used to sample hydrate-entrained sediments from the Sea of Japan in 2013. The maximum coring depth achieved was 32m below sea floor and the system can operate for more than 50 hours on a single deployment

Figure 2.9: The BGS RD2 System being deployed using dedicated Launch and recovery system

2.4 Logging techniques for marine gas hydrate occurrences

2.4.1 Basics and overview of field studies

Dedicated gas hydrate drilling has started with the recognition of the wide-spread abundance of gas hydrate along most continental margins and their potential as future energy resource or a contributor global climate change. Academic drilling for gas hydrates was initially constrained to expeditions conducted under the umbrella of the Ocean Drilling Program (and its following successors Integrated Ocean Drilling Program, 2002-2012, and International Ocean Discovery Program, 2013-2023). Logging

tools and their operation onboard the drilling vessel 'JOIDES Resolution' are provided by contract to Schlumberger, the leading European provider of technology for the oil and gas industry.

The first dedicated wire-line logs for gas hydrates were acquired during ODP Leg 146 (Westbrook et al., 1994) and ODP Leg 164 (Paull et al., 1996) with the recognition of elevated *p*-wave velocity and electrical resistivity values as primary proxies for the occurrence of gas hydrate (e.g. Collett and Ladd, 2000; Collett and Lee, 2012). After ODP Leg 204 (Tréhu et al., 2003) and IODP expedition 311 (Riedel et al., 2006) along the southern and northern Cascadia margin, a series of semi-industrial drilling expeditions were conducted mostly for exploration of gas hydrates as an energy resource: (1) US Gulf of Mexico, Joint Industry Project (e.g. Ruppel et al., 2008; Collett and Boswell, 2012, and references therein), (2) Japan, Nankai Trough (e.g. Tsuji et al., 2009; Fujii et al., 2009) with the culmination in the first marine gas hydrate production test (e.g. Yamamoto et al., 2014; Yamamoto and Ruppel, 2015), (3) India, off the east and west coast of the Indian sub-continent (two expeditions in 2006 (e.g. Kumar et al., 2014; Collett et al., 2014) and in 2015 (e.g. Kumar et al., 2016)), (4) China, along the South China Sea (four expeditions between 2007 and 2016 (e.g. Shengxiong et al., 2017), see e.g. Matsumoto et al., (2011) and references therein), and (5) Korea, Ulleung Basin (two expeditions in 2007 and 2010, e.g. Ryu et al., 2013). These expeditions often adapted the same procedures for gas hydrate drilling, coring, and logging as developed by ODP and IODP (as e.g. described in Collett et al., 2014; Ryu et al., 2013). Operationally, many of these semi-industrial drilling legs were conducted on a contract basis by Fugro (with staff from Holland, UK, and US offices) in conjunction with GeoTek Ltd (UK).

In many of the modern (post-2000) drilling expedition, gas hydrate drilling starts with the acquisition of Logging-While Drilling (LWD) logs, often in combination with measurement-while-drilling (MWD) as primary safety control (as initially developed for IODP Expedition 311, Riedel et al., 2006). These LWD data are then used as the basis to develop coring and additional wire-line (WL) logging programs including vertical seismic profiling (VSP). Below, LWD, WL, and the VSP techniques are described and a general assessment of the different techniques with resolution limits and pitfalls are given. The ultimate use of the log-data is in a site-by-site core-log-seismic integration (e.g. Bahk et al., 2013a,b; Tréhu et al., 2004; Fujii et al., 2009), seismic inversion (e.g. Lu and McMechan, 2004; Bellefleur et al., 2006), and as ground-truth for basin-wide resource assessments (e.g. Collett, 2004; Frye, 2008). Approaches to drilling and logging in non-marine, i.e. permafrost environments, are often similar to marine environments, but operational challenges require special borehole conditioning efforts. Details on these issues can be found e.g. in Goldberg et al., (2010), Dallimore et al. (1999), Dallimore and Collett (2005), or Collet et al., (2011).

2.4.2 Basic logging methods/proxies for gas hydrate

The most commonly used logs to identify (and quantify) gas hydrates include *electrical resistivity*, *p*-wave and *s*-wave velocity (also referred to as *sonic logs*), and *resistivity- imaging logs* (e.g. Goldberg, 1997; Goldberg et al., 2010; Collett and Lee, 2011; 2012). Additional logs, such as electromagnetic (e.g. Sun and Goldberg, 2005) and nuclear magnetic resonance (e.g. Kleinberg, et al., 2005), are used but are less common. *Porosity*, *density*, and *natural gamma-ray logs* are usually acquired combined with the above standard log-suite, but are only to be seen in the context of the basic-log data and core measurements to provide physical properties of the host-sediments containing gas hydrates. *Electrical*

resistivity logs often rely on the use of Archie's equation (Archie, 1942) linking porosity of the sediments to the formation resistivity with the aim to detect gas hydrates (that act as electrical insulator in the sense of a pore-filling material), thus increasing the formation resistivity significantly above a (site-specific) background trend. Electrical resistivity logs can be acquired with various tools (see e.g. Goldberg et al., 2010 or the ODP logging manual (2004) for details). Borehole imaging is a technique in which the electrical resistivity of the borehole wall is measured and displayed as unwrapped image data. These image data are useful to detect gas hydrate in fractures and are also exploited for structural analyses of the fracture network and stress regime (e.g. Janik et al., 2004; Cook et al., 2008) *Velocity/Sonic* (*p*- and *s*-wave) logs are based on measuring the travel time of an emitted sonic pulse between a source and a series of receivers mounted on the drill/log string. Sonic data are less sensitive to the presence of gas hydrates (especially at low concentrations) than electrical resistivity logs, but elevated *p*-wave velocity values are often used to estimate gas hydrate saturations (e.g. Guerin et al., 1999; Shankar and Riedel, 2011). It should be noted that LWD and WL log data are susceptible to anisotropy in fracture-dominated environments (e.g. Cook et al., 2010). Most log data are naturally measured in a "vertical sense" between pairs of source- and receivers along the drill string. With the semi-vertical fracture network seen in some gas hydrate bearing settings (such as cold vents), measurements of resistivity and *p*-wave velocity are affected and yield artificially higher values and gas hydrate saturation estimates are too high and need to be corrected for this anisotropic effect (e.g. Lee and Collet, 2010; 2013). *Porosity* logs (measured with a neutron source) provide a basic measure of formation properties used to deduce gas hydrate saturations. Porosity is a basic input parameter for the Archie equation as well as the rock-physics model used for *p*- and *s*-wave velocity log data. *Density* logs measure the sediment bulk density by using a radioactive Cesium source and using Compton scattering and photo-electric absorption to link electron density of rocks/sediments to bulk density. If grain-density is known, the density-log can be converted to an independent porosity-log. *Natural Gamma ray logs* are measuring (passively) the natural gamma ray intensity of the sediments. Data are useful for sediment classification and sand-detection, but also as simple tool to detect borehole enlargements.

2.4.3 LWD and MWD operation

LWD tool strings can be operationally complex, and can be combined with different tools to make up a tool string often more than 30 meter in lengths. The basic advantage of LWD operations is that physical properties are measured directly during drilling (borehole advancement) and thus, sediments have not been significantly altered from the drilling process itself. The use of LWD is especially important for detecting gas hydrates, as the quality of wire-line logs may be hampered as the drilling (and coring) process could have resulted in gas hydrate dissociation, gas release from below the base of hydrate stability, or formation damage (hole enlargements). LWD was first implemented for gas hydrate research only during ODP Leg 204 in 2002 (Tréhu et al., 2003), but has since then become a standard part of all subsequent gas hydrate drilling operations. LWD data offer several other advantages: full 360° borehole coverage (e.g. for imaging and fracture detection), information of hydrate distribution prior to coring to optimize the use of special coring tools (e.g. pressure cores) or other downhole measurements (e.g. temperature or pressure), as well as providing direct means for

assessing drilling safety through the use of measurement-while-drilling (MWD) tools, that pulse log-data up the borehole to the rig-floor for immediate data recovery (though at a reduced sample rate).

2.4.4 Wire-line logging operation

Wire-line logging is used after a borehole has been drilled (and/or cored) and tools are inserted into the borehole using a separate wire-line for continuous measurements of the physical properties of the sediments. It should be noted that wire-line logging is typically depth-limited (as described below) to ensure drilling safety and tool-recovery. Wire-line logging tools used during the ODP and IODP programs are described in the ODP Logging Manual (2004). The "standard" tools deployed for a complete log-suite comprise the triple-combo (consisting of tools to measure natural gamma, porosity, density, resistivity, and borehole diameter or caliper) and the Formation-Micro-Scanner (FMS)-sonic tools (consisting of tools to measure natural gamma, shear- and *p*-wave velocity, and to acquire borehole resistivity images), combined sometimes with the well-seismic tool (WST) for conducting vertical seismic profiles. WL-tools are typically run from the bottom of the hole upwards. Heave-compensation as part of the wire-line operation ensures that the tool is pulled at a speed to measure the physical properties continuously and in regular depth intervals. In generalized terms WL-tools allow measuring physical properties at higher sampling rates and densities as LWD tools as the deployment speed is often much slower than used for LWD. However, as the measurements are made post-drilling of the borehole, data is highly dependent on hole-size (diameter) and shape. Also, the depth-coverage of WL-deployments is smaller than with LWD acquisition as the WL-tools are deployed not from the seafloor but from a suspended drill-pipe up to 60 meter below seafloor. Also, borehole instabilities may result in reducing of the overall borehole depth as tectonic forces or instable sediments fill the bottom of the hole gradually. Conditioning of the borehole (so called wiper-trips) may mediate this effect and the use of special borehole fluids (e.g. guar-gum, oil-based drill-muds, or heavy drill mud) may overcome these problems. However, the use of heavy mud increases the risk of artificially fracturing the formation, if the drill mud is heavier than the surrounding sediment yield strengths.

2.4.5 Vertical Seismic Profiling

One of the fundamental problems in geophysical imaging of gas hydrate is related to the different acquisition domains of the geophysical tools: seismic surveys image the subsurface and are acquired in time-domain. They can be depth-migrated, but velocity functions are often very smooth and coarsely sampled. Logging (and coring) is done by directly measuring data inside the borehole as function of meter below rig-floor (which due to heave-compensation of the drill string) is easily converted to meter below seafloor (mbsf). In order to provide a direct conversion of depth (in mbsf) to two-wave travel time (TWT) of the seismic data, so called check-shot or vertical seismic profile surveys are carried out. These surveys are based on deploying geophones inside the borehole (i.e. the WST) that are mechanically clamped to the borehole wall while emitting a sound source at the sea-surface above the borehole, typically with a single airgun deployed from the drill ship. The direct travel path of the seismic waves emitted are detected at the geophone and the airgun shots are repeated

per station until a stable measurement is achieved, followed by shifting the geophones inside the borehole to another depth interval. The WST tools may contain only a single geophone, but often a string of geophones is used for efficiency of the measurements. As the mechanical clamping of the geophones to the borehole wall damages the formation, the VSP is usually the last wire-line operation in a borehole. VSPs have been applied to almost all gas hydrate drilling during ODP, IODP Legs or other national hydrate drilling programs (e.g. Holbrook et al., 1996; Pecher et al., 1997; Tak et al., 2013) or Arctic drilling expeditions (Milkereit et al., 2005; Sakai, 1999; Walia et al., 1999). An extension of the VSP is possible by shooting the airgun at farther offsets from the borehole, so-called walk-away VSPs (e.g. Pecher et al., 2003; Milkereit et al., 2005). These surveys are demanding as a second vessel is required for conducting the airgun operation. However, walk-away VSPs are a powerful tool for advanced geophysical imaging of the gas hydrate reservoir and to extract additional properties of the sub-seafloor formation, foremost *s*-wave velocities (e.g. Pecher et al., 2010).

2.5 Pressure coring and core-analysis devices

As part of the Japanese government decision to expand the gas hydrate production research to deepwater conditions of Nankai Trough, pressure core sampling and analysis were considered as part of the logging program. These investigations were recently reported by Yamamoto (2016): In the program the pressure-core analysis and transfer system (PCATS) were used. These tools were developed as part of the European HYACE and HYACINTH projects (Schultheiss et al, 2009). Note that there were certain issues with compatibility between the European equipment and the supporting Japanese equipment, and certain devices and adjustment had to be made (Yamamoto, 2016). Core sampling took place in 2012 in Nankai Trough, between depths of 270 to 330 m below seabed. 15 cores of 3.5 m were extracted, out of which 7 lost pressure. The cores were placed in ice-water on board. Nondestructive X-ray scanning, *p*-wave velocity and gamma ray density measurements were performed on the cores. Both onboard and post-cruise tests were performed on the core samples. Fig. 2.10 shows the various investigation performed onboard and post-cruise, as reported by Yamamoto (2016).

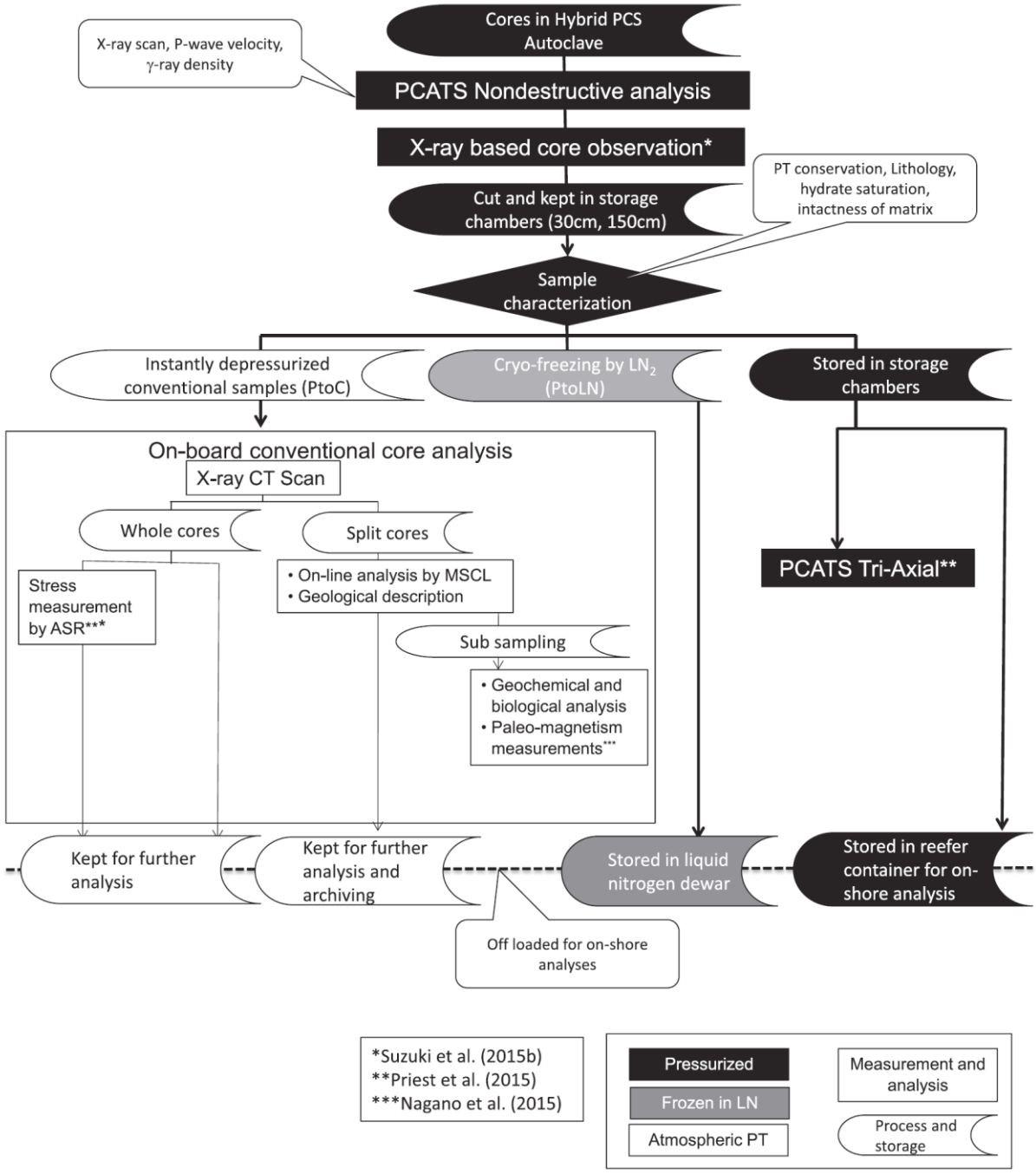

Figure 2.10: Flowchart of test and analyses performed on PCATS core samples (Yamamoto, 2016).

Most interesting, from geomechanics point of view, are the PCATS Tri-Axial tests (Fig. 2.11). In these tests, a short undisturbed sample is transferred from the core into a triaxial apparatus without any hand-touch under the in-situ pressure conditions. The apparatus allows for both small strain and large strain geotechnical testing, as well as direct flow measurements of permeability (Priest et al., 2015).

The system allows for testing under hydrostatic (pressure cell) of 25 MPa. It is composed of several interconnected sections: (*i*) the lower motor driven manipulator which pushes the sample from the (*ii*) Trixial transfer vessel (TTV) to a membrane and then to the (*iii*) test cell, against an upper (*iv*) motor-driven manipulator. The apparatus is capable of performing a Resonance Column (RC) test by torsional vibrations with strain smaller than 10^{-4}, providing (through analysis) the small strain (elastic) shear stiffness, G_{max}. For large strain shearing, the system allow independent control of the pressure cell, water pressure and deviator stress. Control degassing is also possible with evaluation of methane mass. Gradient induced vertical flow through the soil sample allows evaluation of the sediment permeability.

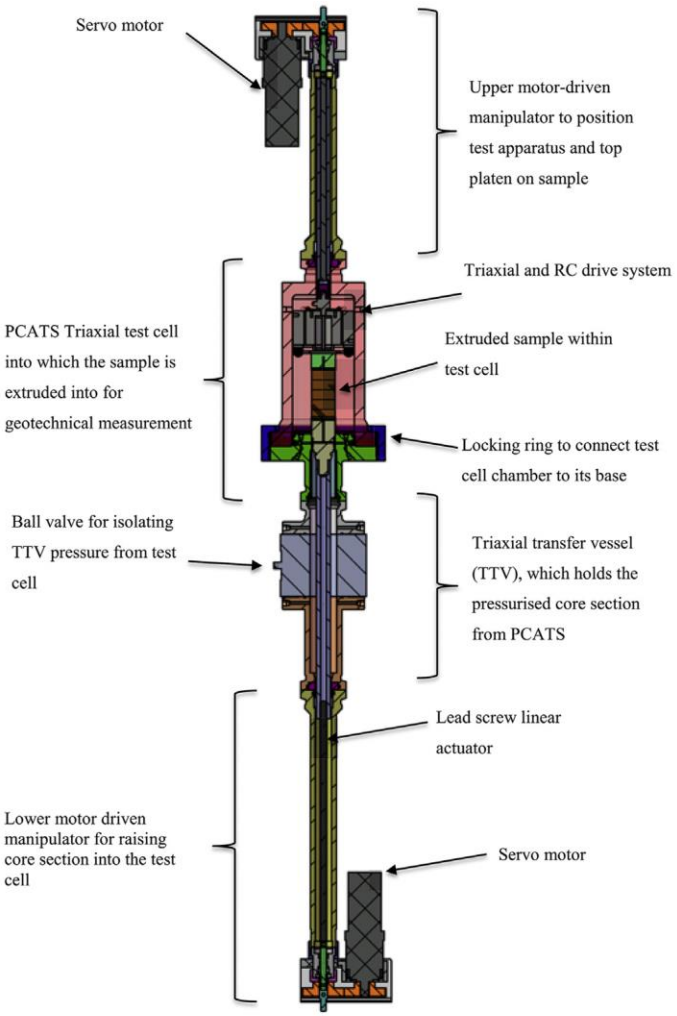

Figure 2.11: Schematic representation of the PCATS Triaxial (Priest et al., 2015).

2.6 Core analysis and Petrophysics

Core analysis relates the measurable physical properties of relevant lithological parameters like porosity, permeability, hydrate saturation, etc. However, drill cores from hydrate bearing reservoirs are difficult and expensive to acquire with preserved in-situ conditions. Furthermore, they cannot

provide the complete picture of the dependencies of physical properties on hydrate saturation as would be possible from geophysical field measurements. Therefore, a number of European research centers have been trying to provide relationship between measurable physical properties and hydrate saturations in different conditions, using various techniques, among which are:

- In GFZ:
    - SEPP, which can measure electrical impedance from mHz to 4 MHz and the sonic wave velocity on hydrate bearing samples (diameter 30mm, length up to 60mm), where hydrate is formed from ice.
    - LARS which can provide hydrate-bearing sediments from methane dissolved in water up to saturations of 90% for production experiments on a dm-scale (diameter 46 cm, length 135cm); it allows to monitor the hydrate generation phase and the production experiment with electrical resistivity tomography (ERT) and seismic wave tomography (SWT)
- In the national oceanography center at Southampton:
    - An ultrasonic rig which measures the sonic properties in ultrasonic frequency and resistivity at 80 Hz. It can use sample of 5cm in diameter and 2cm in radius. Hydrate can be formed using both excess gas and excess water method.
    - Pulse Tube which can be used to measure *p*-wave velocity and attenuation in a frequency range of 3 KHz to 10 KHz. It can contain and handle bigger samples of approximately 6-7 cm in diameter and 0.66 m in height. The resistivity measurements are still to be implemented in this.

3 Production technologies

3.1 General

The formation of marine gas hydrates involves the concentration of remarkable volumes of natural gas, such that the dissociation of 1 m^3 of methane hydrate results in the release of 165 -190 m^3 of free gas. The release of gas from hydrates may be induced by one of the following three methods or by their combination: (*i*) increasing the temperature, (*ii*) decreasing the pressure in the geological formation, and (*iii*) chemical activation, notably by CO_2 injection, which exchanges with and releases CH_4 molecules from the hydrate structures. All of these techniques have been shown capable of producing methane in field tests. Depressurization and CO_2 injection are the most promising methods in economic terms, and the latter has the advantage of being an important incentive for Carbon dioxide Capture and Storage (CCS) technology and research.

To date, three successful production field tests have been undertaken in permafrost environments, and one test in marine settings, which demonstrated that methane extraction and production from submarine gas hydrate reservoirs is viable. The Geological Survey of Canada NRCan conducted three international trial projects for gas hydrate production at the Mallik site, Mackenzie Delta, Canada (1998, 2002, 2007/2008), including thermal and pressure reduction experiments. The projects focused on gas hydrates as an environmentally friendly source of energy for North America. An assessment on

geological hazards from gas hydrates and their climate change implication was carried out. In 2012, ConocoPhillips, the US Department of Energy (DOE), and the Japan Oil, Gas and Metal National Corporation (JOGMEC) conducted the Ignik Sikumi field trial at the Alaska North Slope, USA to investigate the potential of CO_2 storage through CO_2-CH_4 exchange technology. The consortium succeeded in demonstrating the feasibility of injecting mixed gas to exchange CO_2 for CH_4. However, they concluded that while the tested technique may have applications in selected settings, depressurization techniques remain the most promising process for methane production. Furthermore, the first deep water test was performed at a depth of 1 km in spring 2013 in order to produce methane from gas hydrate reservoir of 60 m thickness at a sediment depth of 270 m. Using a technique of pressure reduction, the Japanese MH21 Research Consortium (established by the Ministry of Economic, Trade and Industry (METI)) produced about 20,000 m^3 of gas per day over a period of 6 days. A key problem in developing production technologies is poor knowledge of the geomechanics of sediments bearing gas hydrates. This became obvious during generally successful field tests in the Nankai Trough and below permafrost in Alaska, both of which had been severely impaired by sediment mobilization and uncontrolled sand production (see section 3.2.4 for more details). Currently, the required standards and technical inspection systems for such geotechnical investigations do not exist.

Worldwide, different technological approaches for the optimized exploitation of gas hydrate deposits are being evaluated and compared by means of dynamic system simulations and analysis (see section 3.2 for more details).

3.2 Gas hydrate simulators and geomechnical aspects

Gas hydrate numerical simulators are central tools, used within the research community and industry, to both study and simulate gas production methods and to evaluate geotechnical risk associated with hydrate dissociation. Numerical simulations allow for better understanding of the behavior of gas hydrate-bearing sediments during gas extraction and hence constitute a vital step towards realization of long-term gas production for the future. Unlike conventional deposits, modeling and simulation of gas hydrate bearing sediments is far more complicated, as it entails coupled Thermo-Hydro-Mechanical-Chemical (THMC) processes.

Throughout the last decade a significant advancement has been made with respect to various components of gas hydrate simulators. This section overviews different aspects involved in simulators, with specific emphasis on the geomechnical aspects including the various test methods.

One may identify the various components involved in Gas hydrate bearing sediments simulators and the associate field to which they relate, as provided in Table 3.1.

Table 3.2 mark a few notable simulators used for hydrate production together with identification of the main features involved in the simulator. As can be seen, only 3 simulators include features of mechanical deformation, either through direct coupling or by semi-coupling, as demonstrated in the flowcharts shown in Figs. 3.1 and 3.2.

The following subsections focus on the required elements within the mechanical component aiming for representation of the deformation and yielding of gas hydrate bearing sediments.

Table 3.1: Components involved in gas hydrate simulators and the relevant research field.

Component	Description	Discipline and Research field
Two phase flow (Hydro)	Retention curves, permeability models.	Hydrology/ Soil physics / Fluid mechanics / Petroleum Engineering.
Thermal flow (Thermal)	Thermal conductivity models;	Petroleum Engineering
Hydrate Dissociation (Chemical)	Hydrate equilibrium pressures and temperatures; energies for phase transitions; Kinetic expressions for gas hydrate and gas reactions.	Chemistry and Chemical Engineering.
Deformation and yielding (Mechanical)	Stiffness; strength and yield function; plastic flow; stress relaxation; sand migration.	Geotechnical Engineering

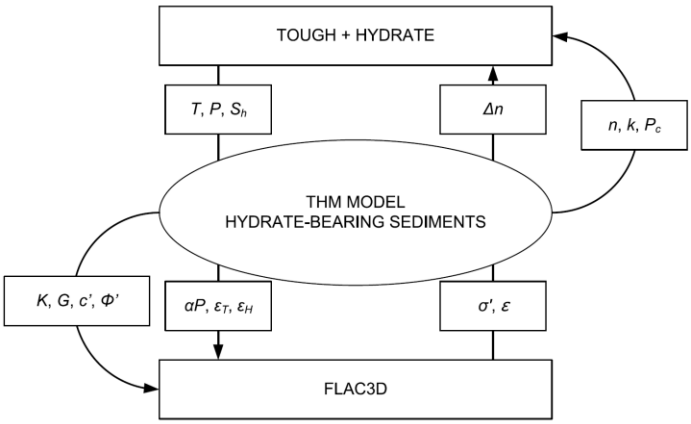

Figure 3.1: Fluid-thermal-mechanical coupled model of TOUGH-HYDRATE & FLAC semi-coupled simulator.

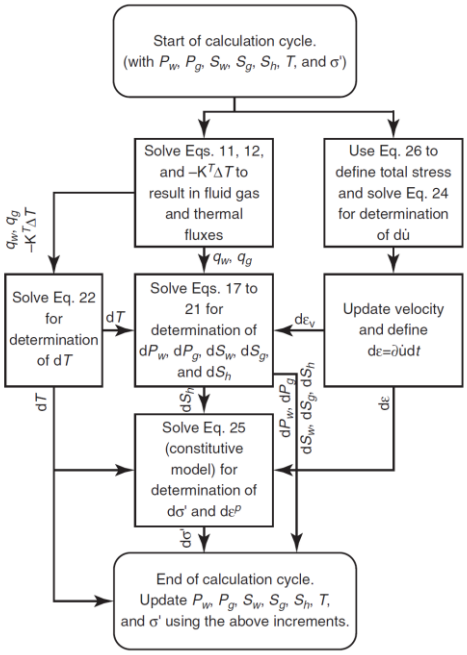

Figure 3.2: Flow chart of a single timestep in the explicitly coupled simulator of Klar et al. (2013).

Table 3.2: Simulators for gas hydrate bearing sediments.

Simulator	Fluid	Thermal	Deformation	Sand migration
TOUGHT-HYDRATE[1]	Yes	Yes	No	No
MH21-HYDRES[2]	Yes	Yes	No	No
STOMP-HYD[3]	Yes	Yes	No	No
TOUGH-HYDRATE & FLAC[4]	Yes	Yes	Semi-coupled	No
Klar and Soga (2005,2010)[5,6]	Yes	No	Yes	No
Kimoto et al. (2010)[7]	Yes	Yes	Yes	No
UMSICHT HyReS[8]	Yes	Yes	No	No
Klar et al. (2013)[9]	Yes	Yes	Yes	No
Gupta et al. (2015)[10]	Yes	Yes	Yes	No
Uchida et al. (2016)[11]	Yes	Yes	Yes	Yes
Qorbani and Kvamme (2017) [12]	Yes	Yes	Yes	No

[1] Moridis, G. J. (2003). Numerical Studies of Gas Production From Methane Hydrates. SPE Journal, 8(04), 359–370

[2] Kurihara, M., Sato, A., Funatsu, K., Ouchi, H., Yamamoto, K., Numasawa, M., … Ashford, D. I. (2010). Analysis of Production Data for 2007/2008 Mallik Gas Hydrate Production Tests in Canada. In *International Oil and Gas Conference and Exhibition in China*. Society of Petroleum Engineers.

[3] White, M. D., & Oostrom, M. (2006). STOMP Subsurface Transport Over Multiple Phase: User's Guide. Pacific Northwest National Laboratory, Washington.

[4] Rutqvist, J., & Moridis, G. J. (2008). Coupled Hydrologic, Thermal and Geomechanical Analysis of Well Bore Stability in Hydrate-Bearing Sediments. In Offshore Technology Conference. Offshore Technology Conference.

[5] Klar, A., & Soga, K. (2005). Coupled deformation-flow analysis for methane hydrate production by depressurized wells. In 3rd International Biot Conference on Poromechanics, May 25-27, 2005, Oklahoma City (pp. 653–659).

[6] Klar, A., Soga, K., & Ng, M. Y. A. (2010). Coupled deformation–flow analysis for methane hydrate extraction. Geotechnique, 60(10), 765–776.

[7] Kimoto, S., Oka, F., & Fushita, T. (2010). A chemo–thermo–mechanically coupled analysis of ground deformation induced by gas hydrate dissociation. International Journal of Mechanical Sciences, 52(2), 365–376. doi:http://dx.doi.org/10.1016/j.ijmecsci.2009.10.008

[8] Janicki, G., Schlüter, S., Hennig, T., Lyko, H., & Deerberg, G. (2011). Simulation of Methane Recovery from Gas Hydrates Combined with Storing Carbon Dioxide as Hydrates. Journal of Geological Research, 2011, 1–15.

[9] Klar, A., Uchida, S., Soga, K., & Yamamoto, K. (2013). Explicitly Coupled Thermal Flow Mechanical Formulation for Gas-Hydrate Sediments. SPE Journal, 18(02), 196–206. doi:10.2118/162859-PA

[10] Gupta, S., Helmig, R., & Wohlmuth, B. (2015). Non-isothermal, multi-phase, multi-component flows through deformable methane hydrate reservoirs. Computational Geosciences, 19(5), 1063–1088.

[11] Uchida, S., Klar, A., & Yamamoto, K. (2016). Sand production model in gas hydrate-bearing sediments. International Journal of Rock Mechanics and Mining Sciences.

[12] Qorbani, K. & Kvamme B. (2017) "Using a Reactive Transport Simulator to Simulate CH4 Production from Bear Island Basin in the Barents Sea Utilizing the Depressurization Method," Energies 10(187); doi:10.3390/en10020187

3.2.1 Main features of the mechanical behavior of gas hydrate bearing sediments

Determination of the mechanical properties of gas hydrate-bearing sediments is an essential prerequisite to evaluate a hydrate accumulation for potential gas production, to predict slope instability, or even methane release. The mechanical behavior is represented in a simulator using a constitutive model, which is the framework which expresses changes in stresses due to strain increments (resulting from deformation). Advanced constitutive models may characterize the global behavior as a whole. However, more often than not, the response is characterized by individual terms and concepts such as elastic stiffness, strength, plastic flow. Fig. 3.3 shows conceptual stress strain and volumetric strain vs shear strain curves as function of hydrate saturation, together with identification of the various terms. Stiffness refers to the ratio of stress increase due to deformation. Strength refers

to the ultimate deviatoric stress (q) that a material can sustain. Dilatancy refers to the material tendency to increase its volume under shearing[1].

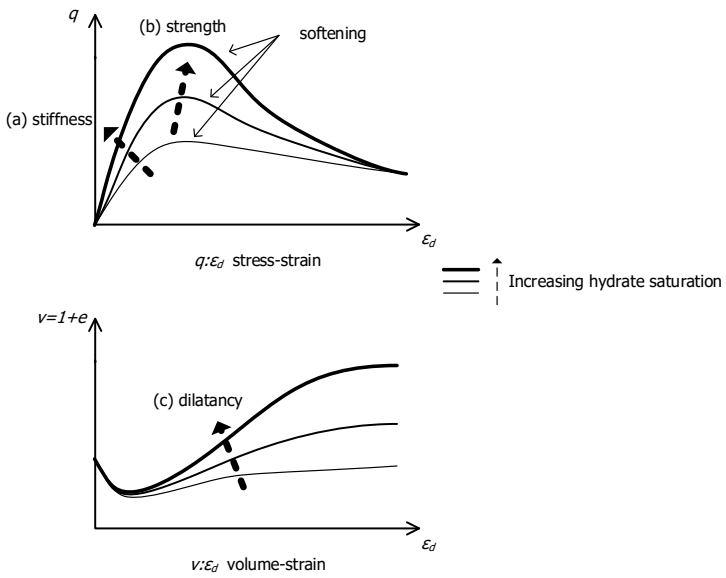

Figure 3.3: Illustration of typical response to gas hydrate bearing sediment to triaxial testing.

These mechanical properties (i.e. stiffness, strength and dilatancy) have been the subject of series of studies over the last decade (e.g. Ebinuma et al., 2005; Priest et al., 2009; Winters et al., 2007; Yun et al., 2007; Santamarina and Ruppel, 2008; Miyazaki et al., 2012; Zhang et al., 2012; Ghiassian and Grozic, 2010, Pinkert and Grozic, 2014). Regardless of the hydrate formation method all have shown the general trends presented in Fig. 3.3.

The existence of hydrate does not only change stiffness, yielding and plastic flow, but also introduces further complexity due to its dissociation. For example, in case the hydrate is stressed (either due to historic events or due to well construction or depressurization) its dissociation will be accompanied by stress relaxation (see Fig. 3.4). The behavior of hydrate bearing sediments under dissociation conditions has not been studied thoroughly in laboratories, nor do all the simulators contain components that represent dissociation induced stress relaxation. Yet, it appears it may be of crucial importance to the overall mechanical behavior of the sediment surrounding a gas hydrate well. For example, Klar et al. (2013) have demonstrated how stress relaxation due to hydrate dissociation leads to a cycle of loading and unloading of shear stresses along interfaces between layers, even if the well depressurization sequence is monotonic. It is speculated that this may also be the reason for the excessive sand production seen in the field trials. This highlights the importance of expanding the laboratory studies for understanding the mechanical response of the material under dissociation process and not only under fixed hydrate saturation. Moreover, methodologies and studies should be developed and carried out to answer the question whether the hydrate is stressed in-situ.

[1] Compaction due to shearing is also relevant. One may view both dilatancy and compaction as kinematic characteristics of the plastic flow (i.e. as plastic volumetric strains due to shearing).

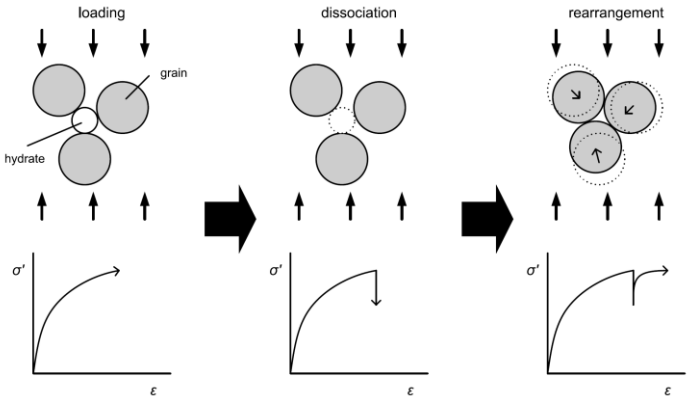

Figure 3.4: Stress relaxation due to hydrate dissociation

3.2.2 Experimental investigations of geo-mechanical properties

The various properties mentioned in section 3.2.1 (e.g. stiffness, strength, and dilatancy) are commonly investigated and studies using artificial hydrate-bearing specimens, due to the high cost and complication involved with extraction of undisturbed samples. Laboratory formation of hydrate-bearing soils has the advantage that it allows repeatable and well characterized sample compositions. Although hydrate can be formed under controlled laboratory conditions, there is still uncertainty with respect to the hydrate growth pattern, its distribution, and in-situ stresses within natural sediments. Therefore, various laboratory hydrate formation techniques have been adopted in different investigations, each of which describes different micromechanical interaction between the hydrate and the soil skeleton, in which the hydrate grows either in the grain contacts or randomly within the pore space.

Existing laboratory hydrate formation techniques, involved in sample preparation for mechanical testing, may be divided into 3 main groups: (*i*) "Pore filling", (*ii*) "Load bearing", and (*iii*) "Grain contact hydrate". The morphology of each group is illustrated in Fig. 3.5. In the case of pore filling morphology, the elastic stiffness (associated with small-strains and deformation) is hardly affected by the presence of hydrate since the soil particles are free to move and rotate. Nonetheless, with the development of deformation and inelastic behavior, the hydrate particles contribute to the overall mechanical response. In the case of load-bearing morphology, the hydrate supports the soil structure but with only little kinematic constraints on the particle displacement (to rotate). In a grain contact (usually termed cemented[2]) hydrate structure, the hydrate closely interacts with the soil particles and thus creates a significantly stiffer and stronger sediment.

[2] The distinction is made herein results from the recent identification that, from mechanical point of view, the hydrate does not cement the particles, but merely alters their kinematic response to shearing (Pinkert, 2016).

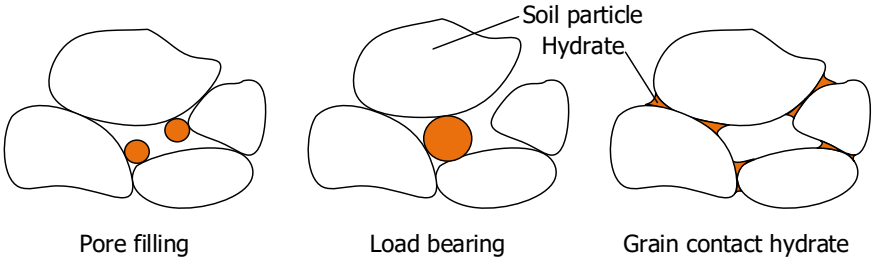

Figure 3.5: Morphology of hydrate formation in artificial soil samples.

Pore filling samples may be obtained by two different preparation schemes. One possible scheme is to form hydrate by injection of water into a sample with an initial limited gas, until the gas is fully dissolved and water pore pressure reached its target back pressure (e.g. Priest et al., 2009). The second approach is to inject gas-water solution (e.g. Tohidi et al., 2001; Yun et al. 2007). Pore filling samples are obtained when the hydrate saturation is below 40%. The same process may be used to create load bearing samples, only with higher concentrations of gas. Alternatively, one may use the ice-seeding approach to form load bearing samples (e.g. Masui et al., 2005; Priest et al., 2005). In the ice-seeding approach, the soil is mixed with crushed ice prior to the sample assembling. While applying the cell and back pressures to the sample, gas is percolated through the sample, resulting in hydrate formation with the water/ice. In the case of "grain contact hydrate", a partly saturated soil is first brought to a certain stress level. Due to capillary forces, water are found near grain contacts, therefore when gas is injected under stable hydrate conditions, hydrate is formed near grain contacts. Clearly, this formation method depends on the grain size distribution and retention curve characteristics. It is believed that pore filling represents best the true morphology of offshore sediments, yet is poses more difficulties than others in the preparation process.

Constitutive models for hydrate-bearing sediment characterization should generally be developed based on large amount of data, which commonly involve test results from various laboratories. In order to obtain comparable test results and reduce their uncertainties, the following aspects should be taken into consideration in sample preparation (hydrate formation method) and documented in detail:

- Hydrate morphology in the pore space.
- Sample homogeneity.
- Thermodynamic conditions.
- Formation time.
- Stress history.

In addition, in order to evaluate the hydrate effect on the hydrate-bearing sediment, proper characterization of an equivalent free-hydrate sample should be carried out, and calculations regarding the hydrate content calculation (saturation) should be clarified with all relevant parameters (e.g., hydrate stoichiometric number etc.).

Laboratory geotechnical investigations are taking place in various institutions around Europe. Table 3.3 lists these laboratories with related capabilities on fields of Geomechanics, Geophysics and Pore-scale observations.

Table 3.3: Laboratories in Europe and capabilities on Geomechanics and Geophysics testing, and Pore-scale observations.

Institute	Country	Geomechanics	Geophysics	Pore-scale observations
University of Southampton	United Kingdom	- Triaxial apparatus - Resonant Column	- Ultrasonic measurements - Resonant Column - Tomography	
Technion IIT (Lab under construction)	Israel	- Triaxal apparatus + double wall cell system - 1D (Oedometric) apparatus	- Ultrasonic measurements	
Ecole des ponts ParisTech	France	- Triaxal apparatus - MRI observations	- Ultrasonic measurements	- X-ray Tomography
Gottingen University	Germany			- X-ray Tomography - Cryo-SEM - Fast X-ray Crystal Size Determination (FXCSD) - Raman spectroscopy
GEOMAR Kiel	Germany	- Flow-through Triaxal apparatus + ERT - Flow-through Triaxial apparatus + X-ray CT	- ERT	- Raman microscopy - MRI - X-ray CT
Helmotz GFZ, Potsdam	Germany	- Direct Shear apparatus	- Ultrasonic measurements - Electrical resistivity	
IFREMER, France	France	- Triaxal apparatus	- Resistivity Tomography	
Physics and Technology, University of Bergen	Norway		- Ultrasonic measurements - Electrical resistivity - MRI	

3.2.3 Constitutive models for hydrate bearing soil

Constitutive laws (or models) are the set of mathematical rules aiming to represent the sediment mechanical behavior in terms of stress changes (increments) due to strain increments and other state variables, such as hydrate saturation, void ratio, stress level etc., $\delta\sigma_{ij} = f(\sigma_{ij}, s_h, e, \delta\epsilon_{ij})$. The main focus of early years studies to identify the hydrate effect on sediment stiffness, strength and dilatancy, related to the common use of elastic-perfectly plastic constitutive laws, in which yielding is represented by a single (fixed in stress space) yield loci answering the Mohr-Coulomb … together with a non-associative flow rule. Yet the experimental data (new and old) hold valuable information that can assist in developing more unified constitutive frameworks. For example, Pinkert and Grozic (2014) used a comprehensive optimization approach over the entire stress strain curve of more than 30 test results to develop and calibrate a unified (deviatoric strain) hardening model that incorporates the effect of hydrate. The advantage of the model is that it recognizes the relative contribution of the hydrate, and hence allows for determination of the behavior based on pre-analysis of sediment skeleton-related parameters using only standard drained triaxial test results on saturated sand (without hydrate). The model, however, lacks consideration of hydrate induced stress relaxation.

Another good example, is the Methane Hydrate Critical State (MHCS) developed by Uchida et al. (2012). The model follows the ideas of critical state soil mechanics (Roscoe et al., 1958), which represents soil strength and stiffness by deviatoric and volumetric yielding. The model was found to reasonably represent the geomechanical behavior of both hydrate-bearing and hydrate-free sediments as shown in Fig. 3.6.

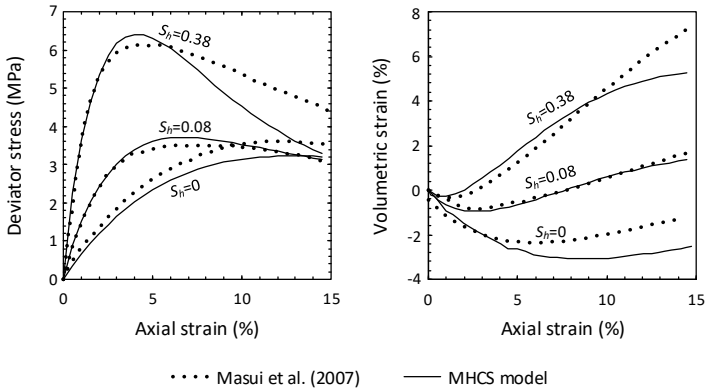

Figure. 3.6: Drained triaxial tests on Nanaki hydrate-bearing sediments conducted by Masui et al. (2007) and the MHCS model simulations.

The key features of the MHCS model are: (*i*) to incorporate the strength enhancement due to hydrates by enlargement of the hydrate-free yield surface, which implicitly induces a greater dilatancy; (*ii*) to represent smooth transition from linear-elastic to plastic behavior; (*iii*) to capture shear-induced degradation of the geomechanical contribution from hydrates; and (*iv*) elastic stiffness increase due to hydrates. The model has been further developed by other researchers to include the effect of the intermediate principal stress (Lin et al., 2015) and state-dependent dilatancy equation (Shen et al., 2016).

Another interesting approach has been developed in Barcelona, in which a unified critical state model CASM (Clay and Sand Model; Yu, 1998) is adopted for hydrate bearing sand representation, due to its simplicity and flexibility in describing the shape of the yield surface and its ability predicting the mechanical behavior of sands. CASM is formulated in terms of the state parameter concept introduced by Been and Jefferies (1985) and uses the stress-dilatancy relationship proposed by Rowe (1962).

The changes in the mechanical properties of the sediment due to hydrate is included as a densification process in CASM. This densification process is proportional to hydrate saturation and results in a decrease of the available porosity and increase in the sediment composite bulk moduli. Hydrate-CASM considers changes on sediment properties via (*i*) variation of the initial available void ratio, (*ii*) decrease of the swelling line slope, (*iii*) reduction of the state parameter value, and (*iv*) a widening of the size of the yield surface. The subloading concept (Hashiguchi, 1989) has also been implemented in the formulation to consider plastic deformations inside the yield surface, and to provide a smooth transition from elastic to elasto-plastic behavior.

Hydrate-CASM has been validated against triaxial test experimental data. The model reproduces fairly successfully key features of synthetic methane hydrate bearing sediments (MHBS) mechanical behavior, like increases in stiffness, strength, and dilatancy as can be seen in Fig. 3.7.

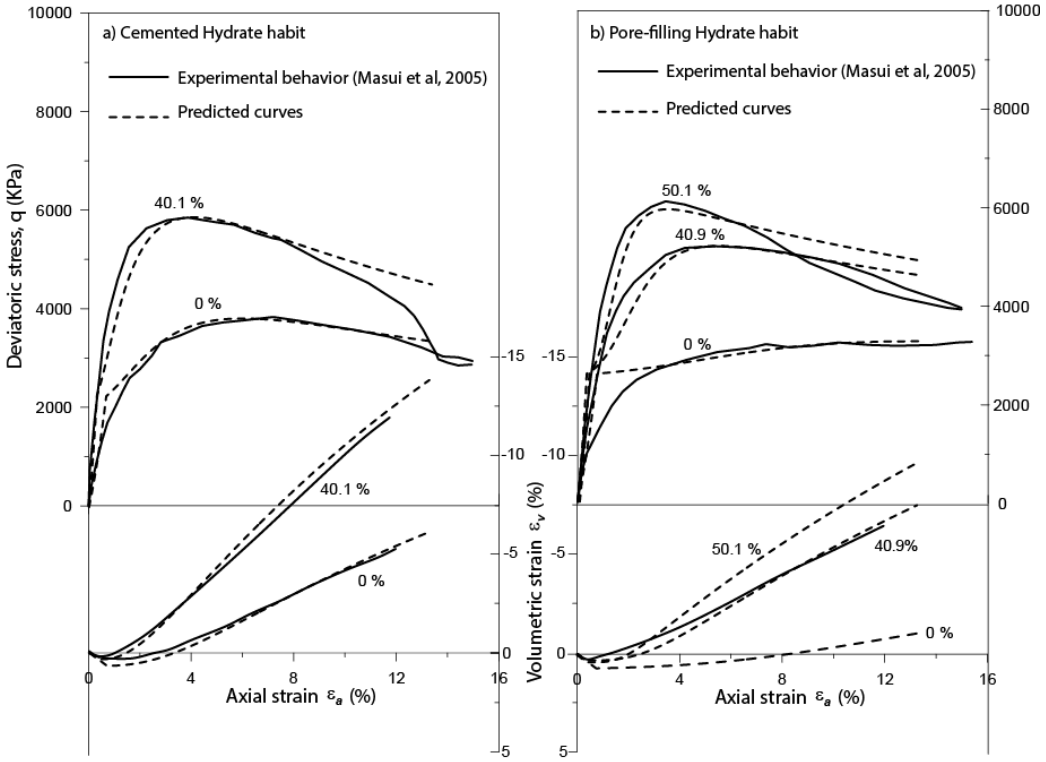

Figure. 3.7: Comparison between Hydrate-CASM predictions and experimental results for synthetic MHBS with different hydrate morphologies: Stress-strain behavior and volumetric response of a) cementing hydrates specimens, and b) pore-filling hydrate specimens, after Masui et al. (2005)

Recently, Pinkert (2016) have also used Rowe (1962) theory and examined its validity for hydrate bearing sands. This theory describes the relation between stresses and plastic flow prior to peak strength. Using the experimental data of Hyodo et al. (2013) and Masui (2005), Pinkert found that, all of the tests results fall on the same line when conducting Rowe stress-dilatancy analysis regardless of the hydrate saturation or formation method (as long as the sand is the same). This indicates that the presence of hydrate merely changes the kinematic of deformation (plastic flow) and does not contribute to the strength in the form of "cohesion" as believed by many. Fig. 3.8 shows the analysis of Pinkert (2016). This finding highlights the importance of understanding the kinematic interaction between hydrate and sediment skeleton, and the need to expand the testing to other conditions than triaxial compression. Based on the earlier recognition of Pinkert (2016) [by private communication], with respect to the non-cohesive nature of hydrate-bearing sediments, Uchida et al., (2016) re-evaluated the MHCS model and found (by a sensitivity analysis and comparison to existing triaxial test data) that the parameters defining the plastic flow are the most dominant ones, suggesting also that

cohesion is not needed in order to fit the experimental results. Lack of true “cohesion” was also discovered independently through direct observation, using CT scans by Chaouachi et al. (2015), as shown in Fig. 3.9.

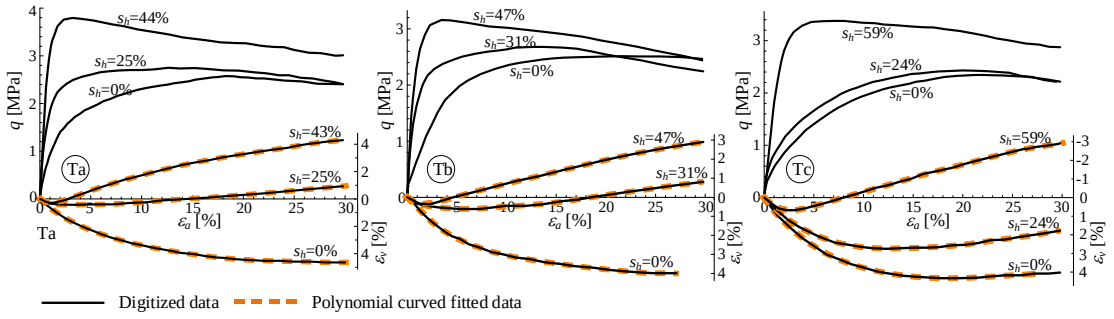

(a)

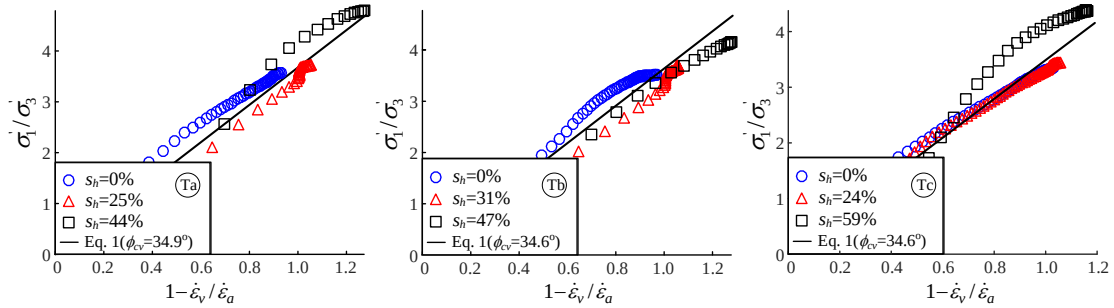

(b)

Figure 3.8: Analysis of Pinkert (2016): (a) Deviatoric stress and volumetric strain versus axial strain in drained triaxial tests of hydrate-bearing Toyoura sands Ta, Tb and Tc; digitized from Hyodo et al. (2013) (solid line) and polynomial curved fitted (dashed line, for continuous derivation purpose); (b) Examination of test results using stress-dilatancy analysis by Rowe (1962) - solid line represents the Rowe expression based on ϕ_{cv} which was obtained from optimization with all hydrate saturations (including zero).

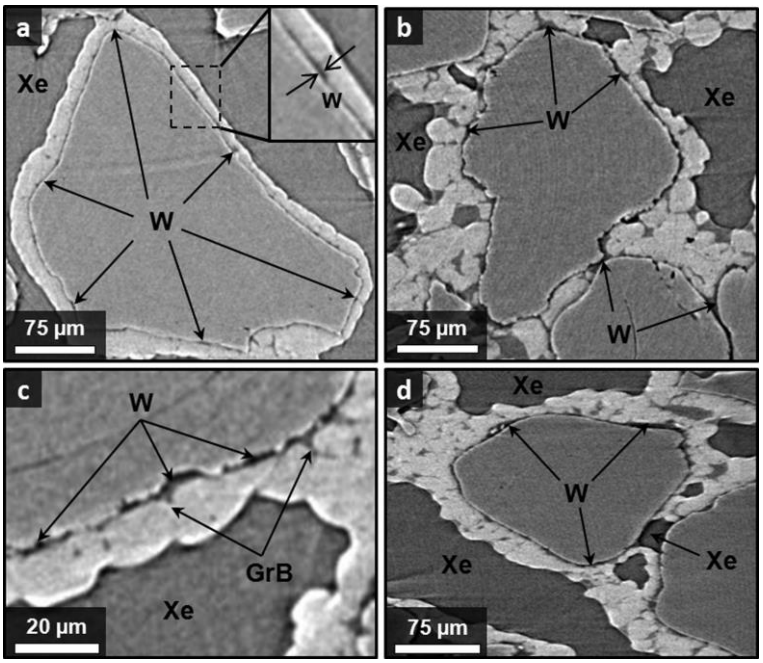

Figure 3.9: CT image showing a thin water layer remaining between gas hydrate (white) and sediment grains; after Chaouachi et al. (2015).

3.2.4 Particle migration

In March 2013, the world's first trial of gas production from offshore hydrate-bearing sediments by depressurization method was conducted at the Eastern Nankai Trough site, Japan. While the operation was successful in producing gas, after six days it suddenly encountered a large amount of sand migration into the well, a phenomenon known as 'sand production', leading to a premature termination of the operation. This incident has highlighted the importance of development of sand migration model within hydrate-bearing sediments for developing of mitigation schemes.

Uchida et al. (2016) provided a comprehensive analytical formulation that entails sand migration problem within gas hydrate-bearing sediments, including features of grain detachment, migration, sediment deformation and hydrate dissociation. The formulation is thermo-hydro-mechanically coupled such that grain detachment causes stress reduction, sediment shear deformation induces grain detachment and grain flow alters multiphase fluid pressure and temperature profiles. Using the developed formulation, the effect of various operational methods on sand production in hydrate-bearing sediments during gas production were investigated numerically. It was found that, out of the different operational methods investigated, lowering depressurization rate was the most effective in reducing sand production for a given gas production.

One exception in which sand production has deceased is the trial at the Ignik Sikumi, Alaska in 2012, which was conducted by chemical activation followed by depressurization. During the trial, initial sand production ceased after two weeks while CH_4 gas production continued for five weeks. The mitigation of sand production was attributed to mechanical or hydraulic effects through the formation of CO_2-rich gas hydrates. This test showed the favorable effect of CO_2 hydrate formation, and highlighted the need to incorporate chemo-processes into existing thermo-hydro-mechanical formulations. Uchida, Deusner, Klar and Haeckel (2016) presented an analytical formulation to capture the coupled thermo-

hydro-chemo-mechanical behavior of gas hydrate-bearing sediments during gas production via CO_2 injection. The key features of the formulation include hydrate formation and dissociation, gas dissolution and multiphase flow for both CH_4 and CO_2, facilitating CH_4-CO_2 hydrate conversion.

3.2.5 Gas hydrates hosted in carbonate sediments

Carbonate sediments comprise the second largest depositional system on earth and accumulate in large quantities in deep pelagic environments and along kilometre-wide marine carbonate platforms that are distal from continental sediment and nutrient flux. Shallow marine carbonate platform environments do not have the pressure/temperature conditions conducive to the formation of gas hydrates. Nevertheless, when these carbonate environments are found in deeper water and colder temperature, conditions become favourable for the formation of gas hydrates. These carbonate prospects have been overlooked although they may hold considerable resources.

In most cases, gas hydrate reservoirs were tested in non-carbonate sediments deposited in offshore river delta environments, e.g., Mackenzie Delta, Bay of Bengal, continental slopes and oceanic troughs (Taiwan, Japan). The sediments in these environments consist of varying proportions of siliciclastic sand (quartz and accessory feldspar grains), clays and some authigenic carbonate. Carbonate sediments have rarely been sampled and tested for the presence of gas hydrates and are generally overlooked as potential gas hydrates exploration targets. To become viable repositories of gas hydrates in areas where biogenic or thermogenic gas has migrated close to the seabed, carbonate sediments need to have porosity and grains size characteristics that are similar to tested non-carbonate sediments as well as conditions where pressure and temperature are conducive to the formation of gas hydrates.

These conditions can be met in unconsolidated to poorly consolidated carbonate sands in the following environments:

1. Drowned carbonate platform: A change in environmental conditions, such as increased nutrient supply and influx of clay or rapid sea-level rise can result in the termination of carbonate production and drowning of the carbonate platform (Gatt & Gluyas, 2012).
2. By-passing of carbonate sand: Carbonate platforms where carbonate production is stimulated and increased by a moderate rise in sea-level. In these cases, carbonate sands are shed to deeper slope environments and troughs during periods of high carbonate production.

Grains in non-carbonate environments (e.g. quartz sand) are usually modeled as well-sorted, rounded to well-rounded spheres with a cubic grain packing that would produce a maximum porosity of 47%. In contrast, typical carbonate sand grains may comprise benthic foraminifera, bivalve, echinoid and coralline red algal clasts which have variable morphologies ranging from spherical, lenticular to irregular-shaped grains with a surface texture that varies from well-rounded to angular. Voids in carbonate grains may include mouldic and intragranular porosity (Figure 3.10). These variable grain morphologies and voids differ from quartz sand fabric and can produce higher levels of porosity and permeability which affect the level of sand production and gas extraction. Carbonate grains may also be deposited in water which is close to carbonate saturation, resulting in early cementation which can have a stabilizing effect in reducing sand production.

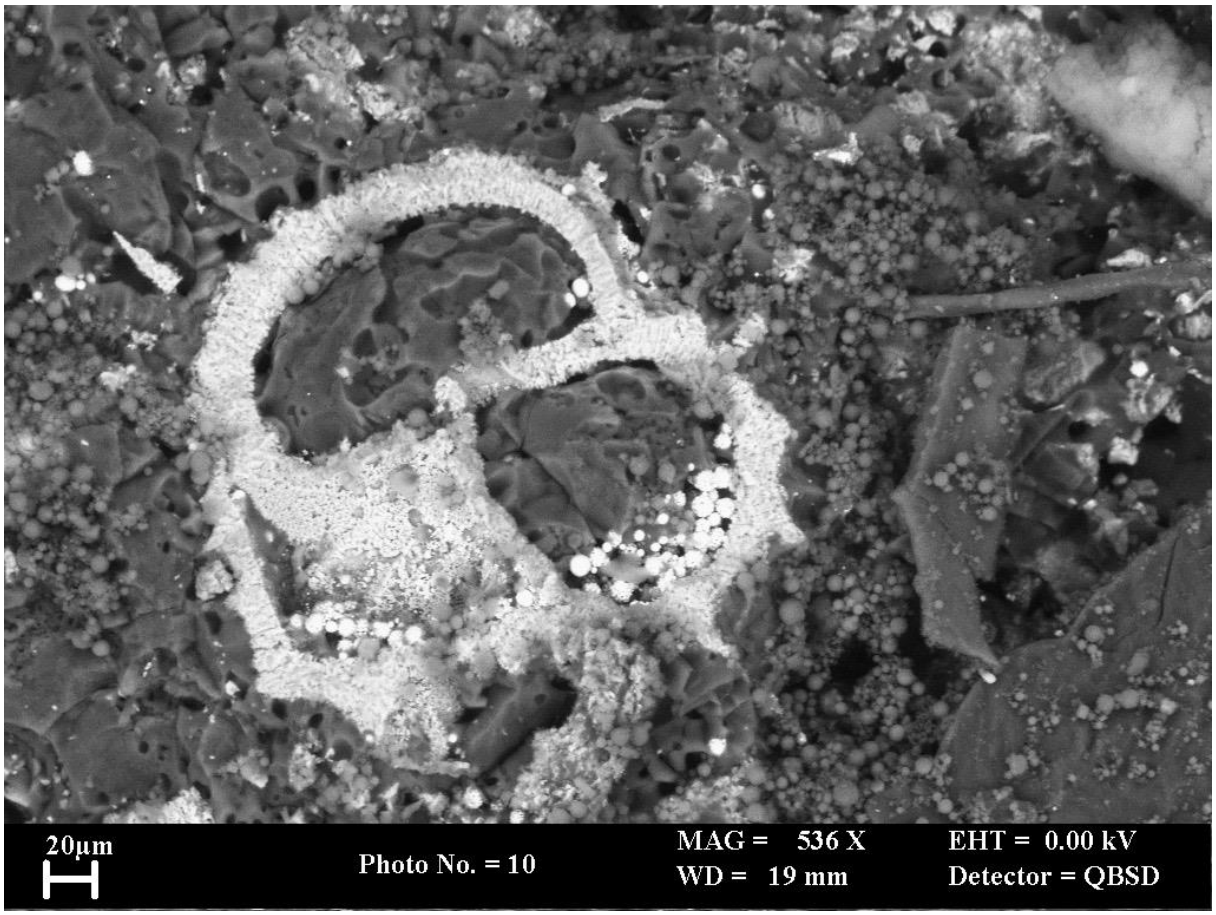

Figure 3.10: Cryogenic SEM photomicrograph of a fractured section through a foraminifera test within sediment (IODP Leg 311, Cascadia Margin, core sample U1327, from approximately 9 m deep in the sdiment). Authigenic pyrite framboids [bright] are present both within the test and in the surrounding ice-mud matrix. Water-ice [dark grey] largely fills the chambers of the test (Rochelle, unpublished information).

4 Monitoring

Technological advancement and increasing environmental awareness have led to an enhanced dissemination of monitoring approaches. Nowadays, monitoring of the environment is considered an essential tool related to the economic, ecologic and safe use of energy resources and its legacies (c.f. CCS legislation, *CCS-directive*, European Parliament, Council of the European Union, 2009), and will apply to methane hydrates as a new energy source as well. Therefore, a comprehensive monitoring scheme is a prerequisite for social acceptance and official permission.

Monitoring activities should ideally be conducted throughout the whole process, starting with vessel-based overview and baseline measurements to find and quantify natural seepage during the exploration phase, continuing during drilling and intensifying during exploitation as pointed out in, and defined by, the mining codes for marine mining by the International Seabed Authority ISA (https://www.isa.org.jm/mining-code; last visited 03 May 2017). Even in the post-production phase,

abandonment monitoring is an important task to detect environmental hazards at an early stage, i.e. gas ebullition or sediment movement, potentially emerging from the disused production sites.

This section presents a selection of potential multi-parameter monitoring techniques and concepts for continuous monitoring in the water column and at the seabed around a methane hydrate production site. These techniques and concepts match those of scientific-oriented production tests where monitoring still serves to increase the general understanding. Monitoring related to commercial production is, status today, not (legally) defined and might be site-specific.

The following selection neither covers survey based (acoustical) geophysical reservoir monitoring, nor pore water analysis and does not describe borehole monitoring options (i.e. *logging while drilling*) except for an introduction to distributed fiber optic sensing. All of these mark additional monitoring options suitable for answering specific questions on different spatial and temporal scales.

4.1 General

Monitoring of the environment is an essential task when dealing with the economic, ecologic and safe use of sub-marine methane hydrates as a new energy source. Therefore, a comprehensive monitoring scheme is a basic requirement for social acceptance and official permission.

Monitoring activities should ideally be conducted throughout the whole process, starting with vessel-based overview and baseline measurements to find and quantify natural seepage during the exploration phase, continuing during drilling and intensifying during the exploitation and production phase. Even in the post-production phase, abandonment monitoring is an important task to avoid environmental hazards potentially emerging from the disused production sites.

In the following sections, a suitable monitoring concept will be addressed, and technologies, which are used for monitoring in the water column and at the seabed around a methane hydrate field site will be discussed.

4.1.1 Basic Concepts of Modular and Scalable Monitoring Networks

Permanent monitoring systems, deployed on the seabed in a methane hydrate field, are a suitable method to address measuring challenges. As exemplarily visualized in Fig 4.1, several nodes equipped with different sensor suites form a monitoring network at the seabed and communicate with each other. The individual stationary nodes should be placed at characteristic and significant points, which are for example in direct vicinity of the drilling well, where the sediment structure is disrupted due to the drilling process or at natural faults in the hydrate field.

At least one node should be placed outside and upstream every activity of the methane hydrate field (c.f. the upper left node in Fig. 4.1). This reference node will monitor the baseline during the whole process. It is important to decide whether any parameter change detected by the monitoring system around the center of activity is caused by, or originates from, changes of the outer conditions, or if it is due to production action. The latter would point to a potential hazard and requires closer investigations, e.g. by means of triggered and dedicated surveys.

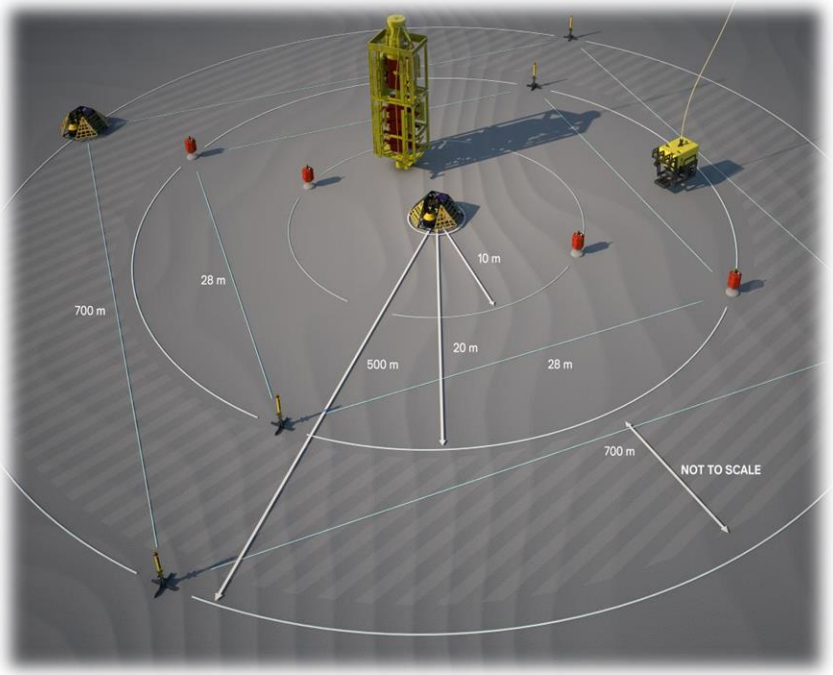

Figure 4.1: Exemplary installation setup of a monitoring network at the seabed (courtesy of Kongsberg Maritime Underwater Positioning and Monitoring, Fietzek et al., 2016).

All data recorded by the network will be collected through a small data processing unit (DPU) mounted on each node. Besides storing the raw data the DPU condenses and interprets the data directly at the sea bed. It is not only communicating with the other nodes of the network by acoustic means, but also with the “topside”, such as a vessel, an unmanned surface vehicle or a buoy, to regularly transmit status information. If the status shows a leakage alarm, the raw data from the relevant node can also be accessed from the topside. All other data will be stored at the seabed and can be used for extended post-processing and interpretation after a recovery of the nodes during maintenance tasks. Data handling and management is an essential step at all levels of an integrated monitoring system. Furthermore, advanced data products from a monitoring system can be generated by transferring their data into site-specific predictive models.

Apart from the reference node(s), the described network is placed in direct vicinity of the production well and in the near field. As shown in Fig. 4.2, also the mid and far field of the reservoir should be included in the monitoring scheme and targeted with reasonable sensor-platform combinations to gather the “full picture” of the hydrate field. Monitoring large areas cannot be achieved by stationary platforms equipped with point sensors alone. Different sensors on submersible mobile platforms like ROVs, AUVs or Gliders are more suitable to monitor water column and sediment surface, because these platforms can flexibly cover lager areas. These measurements can be supplemented by vessel-based monitoring using sonar systems for e.g. gas bubble detection. All these different kind of platforms can be connected and integrated into the monitoring network. All data, independent of its

origin from a stationary monitoring node or a mobile platform survey, should be collected, fused and processed to obtain advanced data products as an output (Fietzek et al., 2016). This finally provides the targeted situation awareness of the environment under investigation.

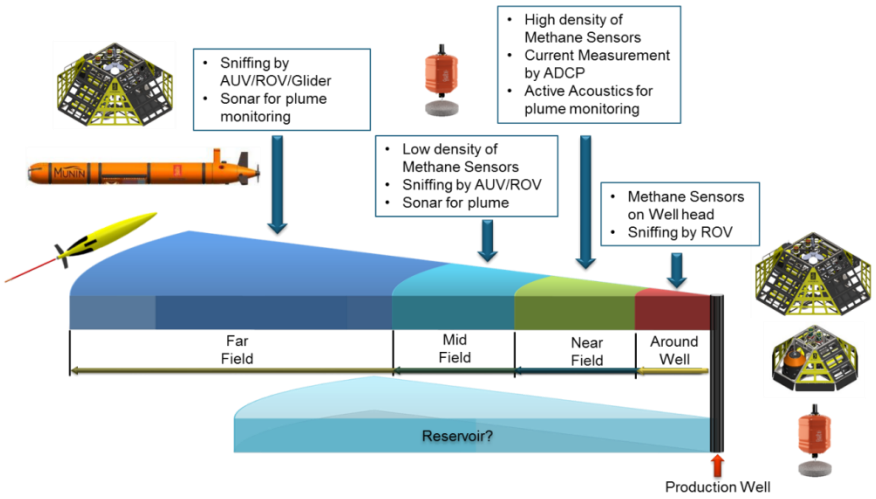

Figure 4.2: Monitoring solutions adapted to the distance from the production well (courtesy of Kongsberg Maritime Underwater Positioning and Monitoring).

4.1.2 Monitoring Technologies - Stationary Lander Systems and Point Sensors

In a lander-based monitoring system, all the proposed nodes are stationary observatories at the seabed and mainly function as versatile carriers for diverse sensors. The landers have a unified design, provide a networking capability, are modular and scalable. Especially at the seabed environmental monitoring represents a great challenge, because all systems need to perform reliably under extreme conditions (high pressures up to several hundred bar), in a cold and corrosive environment and under energy limitation. During a long-term deployment, changes of the environmental factors (e.g. currents) might influence the effectiveness of the monitoring.

Beside sensors, every lander should comprise a DPU for collecting, processing and storing the data as well as acoustic transmitters for communicating with other nodes or the topside, a sufficient quantity of battery packs, and a possibility for safe, reliable and economic launch and recovery. All sensors need to be maintained on a regular (up to yearly) basis and battery packs substituted.

In general, any sensor can be mounted on a lander system and integrated into the monitoring network. Every node or platform can be equipped with different sensors according to the requirements, which were determined in advance, e.g. during a pre-survey of the site. Later adaptations of the payload composition can also be realized during maintenance tasks and the measuring configuration changed by command from the topsite (c.f. preceding section).

To every single sensor on every single node an individual measurement schedule can be assigned, depending on the monitoring challenge for every parameter (e.g. if long-term changes during the

whole production process, seasonal background cycles or a tidal cycle should be monitored) or on its power consumption.

A division into three monitoring tasks (for methane/dissolved gases, environmental condition and deformation) is useful to cover the entire monitoring tasks during gas hydrate production. With respect to methane monitoring, different sensors should be used to determine and quantify gas released into the water column. On the one hand, point sensors for direct measurement of dissolved gases in water (CH_4, CO_2, O_2) are proven state-of-the art technology. On the other hand, active and passive acoustics (hydrophones, sonars, in special cases also echo sounders or cameras) can be used for gas bubble detection in the water column over a larger area. Depending on the monitoring challenge, sonars can be mounted on a lander system for a horizontal scan, or on a surface platform to scan vertically through the whole water column. With respect to the general characterization of environmental conditions at the site, further sensors can be used to evaluate important parameters of the surrounding water, which are essential for correct interpretation of a possible leakage and sediment movement and for generation of a complete environmental model. Sensors of proven technology can be used for this task: oceanographic sensors for physical parameters (CTD), currents (ADCP, current profiler) as well as turbidity, particle size or biological parameters such as chlorophyll fluorescence.

With respect to deformation monitoring, the seabed needs to be monitored with highly accurate methods, since even small deformation and subsidence processes around the production well could be a serious indication of an imminent hazard. Sensors for highly accurate pressure and inclinometer measurements need to be mounted on several lander systems in the hydrate field. With present technology, heading and tilt can be determined with up to approx. 0.1° and 0.05° accuracy respectively. In addition, relative positions in the hydrate field can be determined with an LBL (Long Base Line) acoustic system. A set of nodes at the seabed (at best every node in the field) is equipped with acoustic transponders, between each a baseline is measured. The acoustic range of the transponders is up to 2000 m (presupposed a more or less smooth seabed without any obstacles between the nodes). From the measured distances and by including the pressure measurements, even the smallest seabed deformation and subsidence can be determined at absolute accuracies of less than 2 cm. The greater the number of transponders in the LBL grid, the higher the positioning accuracy. In addition, known or measured sound velocity will help to increase the accuracy of the LBL system as well as a statistical post processing like sensor fusion algorithms for estimation of the covariance (repeatability of the measurements for each node) and noise suppression.

In summary, it can be emphasized that with the current technology a comprehensive monitoring and alert system atop the seabed is available for submarine mining activities. It should further be supported by sub seafloor observations including logging while drilling measurements and acoustic surveys.

4.1.3 Monitoring Technologies – Distributed Fiber Optic Sensing

Distributed fiber optic sensing has become a valuable monitoring tool in petroleum engineering in recent years, and has even been involved in the monitoring of the few field trial tests mentioned earlier, mainly for temperature profiling. This section reviews recent fiber optic sensing developments that originated from the European research community, which may be incorporated into the well design for well integrity evaluation. In specific, this section reviews recent innovations in the field of Brillouin distributed fiber optic sensing of strain. It should be noted that Brillouin scattering may also be used to evaluate temperature changes (as been previously considered).

Strain is a fundamental component of structural mechanics. It provides information on the stress levels in elastic systems and on the cumulative damage and fatigue in elasto-plastic systems. Evaluation of the induced strain in the production well may well be the most helpful measure of well integrity. Brillouin scattering is a nonlinear process (Boyd 2008), in which acoustic phonons interact with a propagating light wave resulting in backscattering. Brillouin scattering may occur spontaneously due to interaction of thermally (and naturally) induced acoustic waves with an incident light wave, or intentionally by stimulating the interaction using a counter propagating light wave. The latter approach, of Stimulated Brillouin Scattering (SBS), has the advantage of stronger scattering, allowing for more precise measurements, as well as application of more advanced interrogation techniques. In principle, both temperature changes and strain (or density) changes affect the Brillouin scattering, and hence can be evaluated by measuring and analyzing (in the time and frequency domain) the backscattered light. A comprehensive state of the art review of various interrogation techniques of Brillouin distributed sensing can be found in Motil et al. (2016). The following are a few innovative improvements, originating from the European research community, associated with increased spatial resolution and dynamic capabilities.

Conventional BOTDA (Brillouin Optical Time Domain Analysis) is limited to a spatial resolution of roughly 1 m, due to constraints on the effective light pulse width. Zadok et al. (2012) have adopted concepts from radar technology, and utilized them to establish a new paradigm of high-resolution sensing. By using high rate, pseudo-random, phase coding of both the Brillouin pump and the probe waves, they were able to restrict the correlation between pump and probe to narrow peaks with arbitrary separation. Fig. 4.3 shows the principle of random access distributed sensing. Fig. 4.1a illustrates the binary phase modulated Brillouin probe wave complex envelope, propagating in the positive z direction (top row). The sign of the optical field randomly alternates in between symbols through binary phase modulation. The bottom row of Fig. 4.3a illustrates SBS pump wave complex envelope, co-modulated by the same binary phase sequence, and propagating in the opposite direction. Fig. 4.3b demonstrates how the product between the pump envelope and the complex conjugate of the signal envelope generate a constant driving force, which prevails at discrete peak locations only (center), in which the two replicas of the modulation sequence are in correlation. Elsewhere, the driving force is oscillating about zero. Fig. 4.3c shows the magnitude of the resulting acoustic field, obtained by temporal integration over the driving force. This technique allows for considerable improvement in the spatial resolution, to the level of 0.01 m.

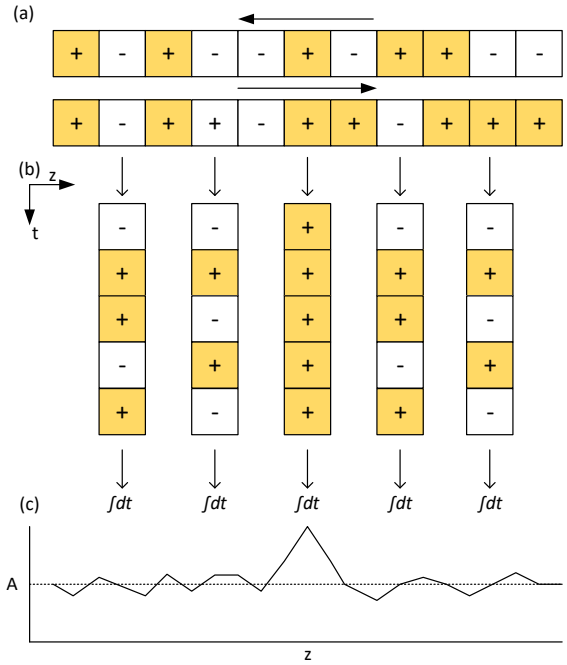

Figure 4.3: Principles of random access distributed sensing. (a) phase modulation of the probe and pump waves; (b) correlation between the coded waves; and (c) the induced acoustic field, allowing for high resolution Brillouin sensing (following Zadok et al. 2012).

Slope assisted BOTDA (Peled et al., 2011), allows for Brillouin based dynamic fiber optic sensing. Rather than evaluating the complete Brillouin gain spectrum (BGS), a single point (i.e. frequency) positioned along the linear, rising or falling, section can be interrogated, thus allowing conversion of amplitude changes to Brillouin frequency changes, as seen in Fig. 4.4. The unique feature of the slope assisted BOTDA is that it allows evaluation of Brillouin frequency dynamic changes for an arbitrary initial Brillouin frequency shift (i.e. for a non-uniformed initially strained fiber). This is achieved by using a variable optical frequency probe wave, whose time evolution is tailored to such that wherever it meets the counter-propagating pump pulse, their frequency difference sits on the middle of the linear part of the local BGS. Peled et al. (2013) were able to demonstrate measurements of strain wave traveling at the speed of 4000 m/s.

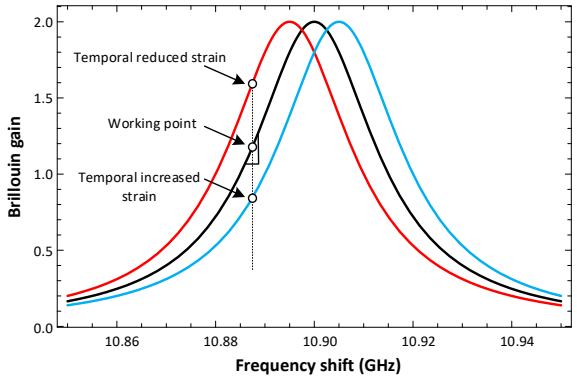

Figure 4.4: Slope assisted Brillouin sensing. A working point, positioned in the center of the linear raising section of the BGS, is selected based on a preliminary BOTDA scanning. Temporal changes in strain shift the BGS left of right. The amount of shift can be evaluated based on the gain change at the working point (consider a linear relation based on the slope), after Peled et al. (2011).

The ability to evaluate strain profiles at high resolution and to investigate dynamic wave propagation within a given structure, facilitates the possibility of developing static and dynamic strategies for wellbore integrity. Stress analysis, similar to that performed within pile foundations (but which relies on the spatially distributed strain profile) may allow investigation of both the well structure integrity and the condition of the surrounding sediment. Static high resolution sensing may infer on stress concentrations and the onset of damage. High resolution distributed sensing may also be incorporated into fundamental laboratory studies of stress strain response of hydrate bearing samples, as was demonstrated by Uchida et al. (2015) for uniaxial loading of acrylic glass.

5 Fundamental (multiscale analytical and experimental) research for future production R&D

Hydrates are complex multi-scale and multi-phase systems that can form from various phases, including water, hydrate formers adsorbed on mineral surfaces, hydrate formers dissolved in water. The number of independent thermodynamic phases is too high to result in any possibility of thermodynamic equilibrium in natural systems. Depending on the origin of the hydrate former, different hydrate structures can form.

This non-equilibrium system depends on mass and heat transport processes from micro-scale to macro-scale. As a consequence, the properties of the material may be changed on a time scale of minutes up to hours and days when samples are collected (for instance when samples are stored and confined in a container). These properties are very dependent on the original local state.

Experiments and modeling on molecular-scale and macro-scale are needed to determine how much the samples (phase distribution in the pore, composition, hydrate phases, saturation, geomechanical properties) will be affected over time upon changing boundary conditions, or by perturbation during recovery or exchange with CO2. Similarly, in terms of mechanical properties, hydrates are hard phases in relative sense similar to minerals when compared to liquid phases and/or gas. It is important to determine how these properties are modified by the confinement. Also, the fluid flow through the pores may affect the compressibility of the pore-hydrates system.

Mineral surfaces structure water in different way depending on the surface distributions of charge atoms. Hydrates former like methane can sometimes be adsorbed inside structured water. In case of polar molecules likes H2S, CO2, direct adsorption on mineral surfaces are also possible. The properties of the adsorbed gas molecules are different from the same molecules in gas phase or dissolved in liquid water.

A complementary scheme of experiments and computer modeling is needed to capture the dynamics of the multi-scale phase transitions involving hydrates, fluids, mineral surfaces and sediments. Fig. 5.1 and Table 5.1 describe complementary techniques designed to probe at distinct spatial resolution from nano-scale to macro-scale or even field. Phase transitions are by nature nano-scale phenomena occurring on a cross interfaces. But associated mass transport is implicitly coupled to higher order transport (micro scale, fluid dynamics, larger scale flow).

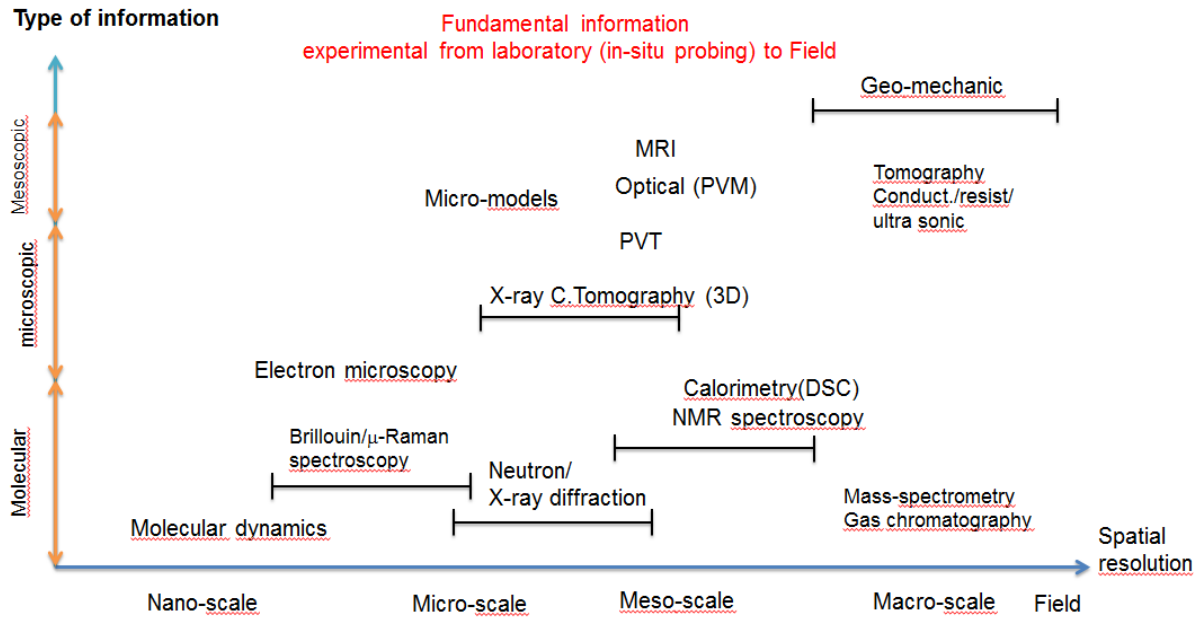

Figure 5.1: Techniques of investigations for gas hydrate research and type of information obtained as a function of spatial resolution

Table 5.1: Experimental techniques used for gas hydrates or gas phase characterization and the type of information obtained, the scale probed and the nature of phase investigated.

Experiments	Scale	Probed	Information
MRI	300 μm		Kinetics/morphology
MS-Chromatography		Gas phase	Composition
NMR-I	~10 μm	Bulk	Composition/Kinetics
Raman Brillouin spectroscopy	< μm	Interface+bulk	Thermo/Kinetic/composition
X-ray diffraction	~ μm to 10 μm	Bulk	Structure/composition
Cryo tomography	~ 5-10 μm	Bulk	3D morpho

From the above figure and table, it is a clear that there is a need for a cross discipline treatment of hydrate bearing sediments, which will reveal the intricate interaction that exists between the various components of the systems at their different scales (molecular, soil grain contact, soil skeleton, and formation layers). Multiscale analytical and experimental research plan may help discover the fundamental mechanisms that govern the system. For example, the validity of artificial hydrate formation in soil testing and its implication on the mechanical response characterization is yet clear and warrants research. Issues of geological history and stressing may be of high interest for future production and may be approached by multiscale cross discipline research. Time scale behavior of the quasi-static and dynamic systems may be of interest, relating hydrate recrystallization rate to geological and production scales.

6 Summary, outlook and conclusions

One of the promising energy resources, capable of answering mankind's energy demands for the next 100 years, is methane hydrate. Throughout the last decade significant research has been conducted on various aspects of gas hydrate, leading also to recent, limited in number, onshore and off-shore production tests. While members of the academia and industry of Europe have been involved in various aspects of the worldwide R&D effort, led by Non-European countries (e.g. Japan, South Korea, USA, China, Taiwan, India, New Zealand), they have never collaborated and worked together to advance and promote production of gas hydrate from European waters.

The migrate project (COST Action ES1405) has taken the first steps towards the creation of a European network that would integrate expertise from European research groups and industrial players with the aim of advancing the potential exploitation of gas hydrate in Europe. As part of this objective, this (first) WG2 report overviewed various aspects related to the production of gas from gas hydrate bearing sediments, with an emphasis on technologies originated from Europe specifically for gas hydrate, and on technologies that could be modified (relatively easy) for the purpose of gas hydrate exploration, monitoring and production. In specific, the use of the *MeBo200* (developed by Bauer Maschinen GmbH and MARUM) as both exploration and production tool may be a valuable solution.

It is clear that Europe holds tremendous capabilities in key areas of gas hydrate research and development (which include: offshore drilling equipment, laboratory testing facilities, numerical simulations, and a range of monitoring technologies). Whilst we acknowledge that many technical hurdles remain to be overcome in terms of successful hydrate exploitation, if we are to demonstrate Europe as a World leader in the exploitation of gas hydrate resource, then we first need to facilitate co-ordination, joint working and information sharing between the many different European groups involved.

7 List of figures

8 List of tables

9 References

Abubakar, A., Gao, G., Habashy, T.M., Liu, J. (2012) "Joint inversion approaches for geophysical electromagnetic and elastic full-waveform data." Inverse Problems, 28, 19 pages.

Archie, G.E. (1942) "The electrical resistivity log as an aid in determining some reservoir characteristics," J. Pet. Technol., 5:1-8.

Attias, E., Weitemeyer, K., Minshull, T. A., Best, A. I., Sinha, M., Jegen-Kulcsar, M., Hölz, S. and Berndt, C. (2016) "Controlled-source electromagnetic and seismic delineation of subseafloor fluid strictures in a gas hydrate province offshore Norway," Geophys. J. Int., 206: 1093 – 1110.

Bahk, J.-J., Kim, D.-H., Chun, J.-H., Son, B.K., Kim, J.-H., Ryu, B.-J., Torres, M., Riedel, M., and Schultheiss, P. (2013a) "Gas hydrate occurrences and their relation to host sediment properties: results from second Ulleung Basin gas hydrate drilling expedition, East Sea, Korea," J. Marine Pet. Geol. 47: 21-29.

Bahk, J.-J., Kim, G.Y., Chun, J.-H., Kim, J.-H., Lee, J.Y., Ryu, B.-J., Lee, J.H., Son, B.K., and Collett, T.S. (2013b) "Characterization of gas hydrate reservoirs by integration of core and log data in the Ulleung Basin, East Sea," J. Marine Pet. Geol. 47: 30-42.

Been, K. and Jefferies, M.G. (1985) "A state parameter for sands," Géotechnique, 35(2): 99-112.

Bellefleur, G., Riedel, M., and Brent, T. (2006) "Seismic characterization and continuity analysis of gas-hydrate horizons near Mallik research wells, Mackenzie Delta, Canada," The Leading Edge, 25(5): 599-604.

Bialas, J. and Brückmann, W. (2009) FS POSEIDON Fahrtbericht / Cruise Report P388: West Nile Delta Project - WND-4. 31, IFM-GEOMAR, Kiel.

Bialas, J. (2013) "3D Seismic and Multidisciplinary Investigations of Cold Seeps along the Hikurangi Margin, North Island, New Zealand," 75th EAGE Conference & Exhibition - Workshops EAGE, London.

Bialas, J., Dannowski, A., Zander, T., Klaeschen, D. and Klaucke, I. (2017) Approaching hydrate and free gas distribution at the SUGAR-Site location in the Danube Delta [Talk] In: EGU General Assembly 2017, 23.-28.04.2017, Vienna, Austria

Boyd, R.W. (2008) "Nonlinear Optics," 3rd ed., Academic press, Waltham.

Breitzke, M. and Bialas, J. (2003) "A deep-towed multichannel seismic streamer for very high-resolution surveys in full ocean depth," First Break, 21(12): 7.

Chaouachi, M., Falenty, A., Sell, K., Enzmann, F., Kersten, M., Haberthür, D., and Kuhs, W. F. (2015) "Microstructural evolution of gas hydrates in sedimentary matrices observed with synchrotron X-ray computed tomographic microscopy," Geochemistry, Geophysics, Geosystems, 16(6): 1711–1722.

Collett, T.S. and Lee, M.W. (2011) "Downhole well log characterization of gas hydrates in nature – a review," 7th International Conference on Gas Hydrates (ICGH 2011), Edinburgh, Scotland, United Kingdom, July 17-21, 2011.

Collett, T. S. and Lee, M. W. (2012) "Well Log Characterization of Natural Gas-Hydrates," Petrophysics, 53: 348–367.

Collett, T. S., and J. Ladd (2000) "Detection of gas hydrate with downhole logs and assessment of gas hydrate concentrations (saturations) and gas volumes on the Blake Ridge with electrical resistivity log data," Proceeding of the Ocean Drilling Program, Scientific Results, 164:179-191.

Collett, T.S. and Boswell, R. (2012) "Resource and hazard implications of gas hydrates in the Northern Gulf of Mexico: Results of the 2009 Joint Industry Project Leg II Drilling Expedition," J. Mar. Petrol. Geol., 34 (1): 1 - 3.

Collett, T.S. and Lee, M. (2005) "Electrical resistivity well-log analysis of gas hydrate saturations in the JAPEX/JNOC/GSC et al. Mallik 5L-38 well," in Scientific Results from the Mallik 2002 Gas Hydrate Production Research Well Program, Mackenzie Delta, Northwest Territories, Canada, S.R. Dallimore and T.S. Collett, eds, Geological Survey of Canada, Bulletin 585, (CD-ROM)

Collett, T.S. (2004) "Alaska North Slope gas hydrate energy resources," USGS Open File report 2004-1454, 6pp, available online at: https://pubs.usgs.gov/of/2004/1454/OFR2004-1454.pdf

Collett, T.S., Boswell, R., Cochran, J.R., Kumar, P., Lall, M., Mazumdar, A., Ramana, M.V., Ramprasad, T., Riedel, M., Sain, K., Sathe, A.V. and Vishwanath, K. (2014) "Geologic implications of gas hydrates in the offshore of India: Results of the National Gas Hydrate Program Expedition 01," Journal of Marine and Petroleum Geology, 58: 3 -28.

Collett, T.S., Lee, M.W., Agena, W.F., Miller, J.F., Lewis, K.A., Zyrianova, M.V., Boswell, R., and Inks, T.L. (2011) "Permafrost-associated natural gas hydrate occurrences on the Alaska North Slope," Journal of Marine Petrolem Geology, 28 (2): 279-294.

Collett, T.S., Lewis, R.E., Dallimore, S.R., Lee, M.W., Mroz, T.H., and Uchida, T. (1999) "Detailed evaluation of gas hydrate reservoir properties using JAPEX/JNOC/GSC Mallik 2L-38 gas hydrate research well downhole well-log displays," In Dallimore, S.R., Uchida, T., and Collett, T.S. eds. Scientific Results from JAPEX/JNOC/GSC Mallik 2L-38 Gas Hydrate Research Well, Mackenzie Delta, Northwest Territories, Canada., Geological Survey of Canada Bulletin, 544: 295-312.

Constable, S., P. K. Kannberg, and K. Weitemeyer (2016) "Vulcan: A deep-towed CSEM receiver," Geochemistry, Geophysics, Geosystems, 17, 1042 – 1064, doi: 10.1002/2015GC006174.

Cook, A. E., Goldberg D. and Kleinberg, R.L. (2008) "Fracture-controlled gas hydrate systems in the northern Gulf of Mexico," Marine and Petroleum Geology, 25: 932–941.

Cook, A.E., Anders, B.I., Malinverno, A., Mrozewski, S. and Goldberg, D.S. (2010) "Electrical anisotropy due to gas hydrate-filled fractures," Geophysics (75)6: F173-F185.

Crutchley, G.J., Maslen, G., Pecher, I.A. and Mountjoy, J.J. (2016) "High-resolution seismic velocity analysis as a tool for exploring gas hydrate systems: An example from New Zealand's southern Hikurangi margin," Interpretation, 4(1): SA1-SA12.

Dallimore, S. R., and T. S. Collett (eds.) (2005) "Initial Results From the Mallik 2002 Gas Hydrate Production Research Well Program, Mackenzie Delta, Northwest Territories, Canada, Geological Survey of Canada," Bulletin 585, 2005; 140 pages (4 sheets); 1 CD-ROM, doi:10.4095/220702

Dallimore, S.R., Uchida, T., and Collett, T.S. (1999) "Summary," in Dallimore, S.R., Uchida, T., and Collett, T.S. eds., Scientific Results from JAPEX/JNOC/GSC Mallik 2L-38 Gas Hydrate Research Well, Mackenzie Delta, Northwest Territories, Canada. Geological Survey of Canada Bulletin, 544: 1-10.

Ebinuma, T., Kamata, Y., Minagawa, H., Ohmura, R., Nagao, J. and Narita, H. (2005) "Mechanical properties of sandy sediment containing methane hydrate," In Fifth International Conference on Gas Hydrates, 958–961.

Edwards, R. N. (1997) "On the resource evaluation of marine gas hydrate deposits using sea-floor transient electric dipole-dipole methods," Geophysics, 62 (1): 63-74.

Ellis, M., Evans, R., Hutchinson, D., Hart, P., Gardner, J. and Hagen, R. (2008) "Electromagnetic surveying of seafloor mounds in the northern Gulf of Mexico," Mar. Pet. Geol., 25(9):960–968.

Fietzek, P., Sobin, J., Kapricheski, P., Meyer, M., Eftedal, T., Nilsen, T. and Themann, S. (2016) "A modular approach to subsea monitoring," International Ocean Systems, 20(2).

Frye, M. (2008) "Preliminary Evaluation of In-place Gas Hydrate Resources: Gulf of Mexico Outer Continental Shelf," Minerals Management Service Report 2008-004.

Fujii, T., Nakamizu, M., Tsuji, Y., Namikawa, T., Okui, T., Kawasaki, M., Ochiai, K., Nishimura, M. and Takano, O. (2009) "Methane-hydrate occurrence and saturation confirmed from core samples, eastern Nankai Trough, Japan," in: T. Collett, A. Johnson, C. Knapp, R. Boswell (Eds.), Natural Gas Hydrates- Energy Resource Potential and Associated Geologic Hazards, AAPG Memoir, 385–400

Gatt, P. A. and Gluyas, J.G, (2012) Climatic controls on facies in Paleogene Mediterranean subtropical carbonate platforms. *Petroleum Geoscience* 18: 355-367.

Gettrust, J.F., Wood, W.T. and Spychalski, S.E. (2004) "High-resolution MCS in deepwater," The Leading Edge, 23(4): 374-377.

Goldberg, D.S., Kleinberg, R.L., Weinberger, J.L., Malinverno, A., McLellan, P.J. and Collett, T.S., (2010) "Evaluation of natural gas hydrate systems using borehole logs," in: Riedel, Willoughby, Chopra (eds.) Geophysical Characterization of Gas Hydrates, 239-261, Society of Exploration Geophysicists, doi: 10.1190/1.9781560802197.ch16

Goswami, B. K., Weitemeyer, K. A., Minshull, T. A., Sinha, M. C., Westbrook, G. K., Chabert, A., Henstock, T. J. and Ker, S. (2015) "A joint electromagnetic and seismic study of an active pockmark within the hydrate stability field at the Vestnesa Ridge, West Svalbard margin," J. Geophys. Res. Solid Earth, 120: 6797–6822.

Gupta, S., Helmig, R., and Wohlmuth, B. (2015) "Non-isothermal, multi-phase, multi-component flows through deformable methane hydrate reservoirs," Computational Geosciences, 19(5): 1063–1088.

Granli, J.R., Arntsen, B., Sollid, A. and Hild E. (1999) "Imaging through gas-filled sediments using marine shear-wave data," Geophysics, 64(3): 668-677.

Ghiassian, H., and Grozic, J. (2013) "Strength behaviour of methane hydrate bearing sand in undrained triaxial testing," Mar. Pet. Geol., 43: 310–319.

Guerin, G., Goldberg, D., and Meltser, A. (1999) “Characterization of in situ elastic properties of gas hydrate-bearing sediments on the Blake Ridge,” J. Geophys. Res., 104: 17781-17796.

Hashiguchi, K. (1989) “Subloading surface model in unconventional plasticity,” International Journal of Solids and Structures 25(8), 917 – 945.

Heincke, B., Jegen, M., Moorkamp, M., Hobbs, R.W. and Chen, J. (2017) “An adaptive coupling strategy for joint inversions that use petrophysical information as constraints,” Journal of Applied Geophysics, 136: 279-297.

Holbrook, W. S., Hoskins, H., Wood, W. T., Stephen, R. A., Lizarralde, D. and Leg 164 Scientific Party (1996) “Methane hydrate and free gas on the Blake Ridge from vertical seismic profiling,” Science, 273: 1840-1843.

Hölz, S., Swidinsky, A., Sommer, M., Jegen, M. and Bialas, J. (2015) “The use of rotational invariants for the interpretation of marine CSEM data with a case study from the North Alex mud volcano, West Nile Delta,” Geophysical Journal International, 201(1): 224-245.

Hu, W., Abubakar, A., Habashy, T.M. (2009) “Joint electromagnetic and seismic inversion using structural constraints,” Geophysics, 74(6): 99-109.

Hustoft, S., Bünz, S. and Mienert, J. (2009) “Three-dimensional seismic analysis of the morphology and spatial distribution of chimneys beneath the Nyegga pockmark field, offshore mid-Norway.” Basin Research, 22(4): 465-480.

Hyodo, M., Li, Y., Yoneda, J., Nakata, Y., Yoshimoto, N., Nishimura, A. and Song Y. (2013) “Mechanical behavior of gas-saturated methane hydrate-bearing sediments,” J. Geophys. Res. Solid Earth 118(10): 5185–5194.

Janicki, G., Schlüter, S., Hennig, T., Lyko, H. and Deerberg, G. (2011) "Simulation of Methane Recovery from Gas Hydrates Combined with Storing Carbon Dioxide as Hydrates," Journal of Geological Research, Article ID 462156.

Jahn, F., Cook, M. and Graham, M. (2008) “Hydrocarbon exploration and production,” 2nd edition Elsevier, Amsterdam.

Janik, A., Goldberg, D., Moos, D., Sheridan, J., Flemings, P., Germaine, J. and Tan, B. (2004) “Constraints on the strength of the gas hydrate-rich sediments from borehole breakouts – implications for slope stability near Hydrate Ridge on the U.S. continental margin off-shore Oregon,” Trans. of Am. Assoc. Petrol. Geol., http://aapg.confex.com/aapg/da2004/techprogram/A88034.htm.

Jing, H. and Xuewei, L. (2011) “A comparison of methods that estimate gas hydrate saturation from well log velocity,” 7th International Conference on Gas Hydrates (ICGH 2011), Edinburgh, United Kingdom.

Judd, A.G. and Hovland, M. (2007) “Seabed Fluid Flow,” Cambridge University Press.

Key, K. (2016) “MARE2DEM: a 2-D inversion code for controlled-source electromagnetic and magnetotelluric data,” Geophs. J. Int. 207: 571 – 588.

Kimoto, S., Oka, F., and Fushita, T. (2010) “A chemo–thermo–mechanically coupled analysis of ground deformation induced by gas hydrate dissociation,” International Journal of Mechanical Sciences, 52(2): 365–376.

Klar, A., and Soga, K. (2005) “Coupled deformation-flow analysis for methane hydrate production by depressurized wells,” In 3rd International Biot Conference on Poromechanics, May 25-27, 2005, Oklahoma City, 653–659.

Klar, A., Soga, K., and Ng, M. Y. A. (2010) “Coupled deformation–flow analysis for methane hydrate extraction” Geotechnique, 60(10): 765–776.

Klar, A., Uchida, S., Soga, K., and Yamamoto, K. (2013) “Explicitly Coupled Thermal Flow Mechanical Formulation for Gas-Hydrate Sediments,” SPE Journal, 18(2): 196–206.

Klaucke, I., Berndt, C., Crutchley, G., Chi, W.-C., Lin, S. and Muff, S. (2015) “Fluid venting and seepage at accretionary ridges: the Four Way Closure Ridge offshore SW Taiwan,” Geo-Marine Letters, 36(3): 165-174.

Kleinberg, R.L., Flaum, C. and Collett, T.S. (2005) "Magnetic resonance log of Mallik 5L-38: Hydrate saturation, growth habit, and relative permeability," in S.R. Dallimore and T.S. Collett (Eds.), Scientific Results from the Mallik 2002 Gas Hydrate Production Research Well, Mackenzie Delta, Northwest Territories, Canada, Bulletin 585. Geological Survey of Canada, Ottawa

Koch, S., Schroeder, H., Haeckel, M., Berndt, C., Bialas, J., Papenberg, C., Klaeschen, D. and Plaza-Faverola, A. (2016) “Gas migration through Opouawe Bank at the Hikurangi margin offshore New Zealand,” Geo-Marine Letters, 36(3): 187-196

Krabbenhoeft, A., Bialas, J., Klaucke, I., Crutchley, G., Papenberg, C. and Netzeband, G.L. (2013) “Patterns of subsurface fluid-flow at cold seeps: The Hikurangi Margin, offshore New Zealand,” Marine and Petroleum Geology, 39(1): 59-73.

Kumar, P., Collett, T.S., Boswell, R., Cochran, J.R., Lall, M., Mazumdar, A., Ramana, M.V., Ramprasad, T., Riedel, M., Sain, K., Sathe, A.V., Vishwanath, K. and Yadav, U.S. (2014) “Geologic implications of gas hydrates in the offshore of India: Krishna-Godavari Basin, Mahanadi Basin, Andaman Sea, Kerola-Konkan Basin,” Journal of Marine and Petroleum Geology, 58: 29 – 98.

Kumar, P., Collett, T.S., Vishwanath, K., Shukla, K.M., Nagalingom, J., Lall., M.V:, Yamada, Y., Schultheiss, P. and Holland, M. (2016) “Gas-hydrate-bearing sand reservoir systems in the offshore of India: Results of the India National Gas Hydrate Program Expedition 02,” in: Fire in the Ice, NETL newsletter, Vol 16, Issue 1, available online at: http://www.netl.doe.gov/File%20Library/Research/Oil-Gas/methane%20hydrates/MHNews_2016_Spring.pdf

Kurihara, M., Sato, A., Funatsu, K., Ouchi, H., Yamamoto, K., Numasawa, M., … Ashford, D. I. (2010) “Analysis of Production Data for 2007/2008 Mallik Gas Hydrate Production Tests in Canada,” In International Oil and Gas Conference and Exhibition in China. Society of Petroleum Engineers. SPE-132155-MS

Kvenvolden, K. (1993) “Gas Hydrates - Geological Perpspective and Global Change,” Reviews of Geophysics, 31(2): 173-187.

Kvenvolden, K. (1988) “Methane hydrate - A major reservoir of carbon in the shallow geosphere?,” Chemical Geology, 71(1-3): 41-51.

Lee, M.W. and Collett, T.S. (1999) “Amount of gas hydrate estimated from compressional- and shear-wave velocities at the JAPEX/JNOC/GSC Mallik 2L-38 gas hydrate research well,” Bulletin of the Geological Survey of Canada (544): 313-322.

Lee, M.W., and Collett, T.S. (2013) “Characteristics and interpretation of facture-filled gas hydrate-An example from the Ulleung Basin, East Sea of Korea,” J. Marine Pet. Geol. 47: 68-181.

Lin, J.-S., Seol, Y. and Choi, J. H. (2015) “An SMP critical state model for methane hydrate-bearing sands,” International Journal for Numerical and Analytical Methods in Geomechanics, 32(9): 969-987.

Liu, X., and P. B. Flemings (2007) “Dynamic multiphase flow model of hydrate formation in marine sediments,” J. Geophys. Res., 112, B03101.

Lu, S., and McMechan, G.A. (2004) “Elastic impedance inversion of multichannel seismic data from unconsolidated sediments containing gas hydrate and free gas,” Geophysics, 69: 164–179.

MacKay, M.E., Jarrard, R.D., Westbrook, G.K., Hyndman, R.D. (1994) “Origin of bottom-simulating reflectors: Geophysical evidence from the Cascadia accretionary prism,” Geology, 22: 459-462.

Marsset, B., Menut, E., Ker, S., Thomas, Y., Regnault, J.P., Leon, P., Martinossi, H., Artzner, L., Chenot, D., Dentrecolas, S., Spychalski, B., Mellier, G. and Sultan, N. (2014) “Deep-towed High Resolution multichannel seismic imaging,” Deep Sea Research Part I: Oceanographic Research Papers, 93: 83-90.

Masui, A., Haneda, H., Ogata, Y. and Aoki, K. (2005) “The effect of saturation degree of methane hydrate on shear strength of synthetic methane hydrate sediments,” in Proceeding of the 5th International Conference on Gas Hydrates, 657–663.

Masui, A., Haneda, H., Ogata, Y. and Aoki, K. (2007) “Mechanical properties of sandy sediment containing marine gas hydrates in deep sea offshore Japan survey drilling in Nankai Trough,” In Seventh ISOPE Ocean Mining Symposium, Lisbon, Portugal, pp. 53–56. International Society of Offshore and Polar Engineers.

Matsumoto, R., Ryu, B.J., Lee, S.R., Lin, S., Wu, S., Sain, K., Pecher, I. and Riedel, M. (2011) “Occurrence And Exploration Of Gas Hydrate,” In The Marginal Seas And Continental Margin Of The Asia And Oceania Region, J. of Mar Petr. Geol., 28: 1751-1767.

Milkereit, B., Adam, E., Li, Z., Qian, W., Bohlen, T., Banerjee, D. and Schmitt, D. R. (2005) “Multi-offset vertical seismic profiling: an experiment to assess petrophysical-scale parameters at the JAPEX/JNOC/GSC et al Mallik 5L-38 gas hydrate production research well,” Bulletin / Geological Survey of Canada ; 585

Moridis, G. J. (2003) "Numerical Studies of Gas Production From Methane Hydrates," SPE Journal, 8(04): 359–370.

Motil, A., Bergman, A. and Tur, M. (2016) “State of the art of Brillouin fiber-optic distributed sensing,” Optics and Laser Technology, 77(A), 81-103.

Miyazaki, K., Masui, A., Sakamoto, Y., Aoki, K., Tenma, N. and Yamaguchi, T. (2011) “Triaxial compressive properties of artificial methane-hydrate-bearing sediment.,” J. Geophys. Res. 116(6): 1–11.

Myer, D., Constable, S. and Key, K. (2010) “Broad-band waveforms and robust processing for marine CSEM surveys,” Geophys. J. Int. 184: 689–698.

Ocean Drilling Program (2004) “ODP logging manual,” available online at: http://www.odplegacy.org/pdf/operations/science/lab_procedures/cookbooks/downhole/logging_manual.pdf, last accessed January 22, 2017

Qorbani, K. and Kvamme, B. (2017) “Using a Reactive Transport Simulator to Simulate CH4 Production from Bear Island Basin in the Barents Sea Utilizing the Depressurization Method,” Energies 10(187); doi:10.3390/en10020187

Paull, C.K., Matsumoto, R., Wallace, P.J., et al. (1996) Proc. ODP, Init. Repts., 164: College Station, TX (Ocean Drilling Program). doi:10.2973/odp.proc.ir.164.1996

Pecher, I. A., Holbrook, W. S., Sen, M. K., Lizarralde, D., Wood, W. T., Hutchinson, D. R., Dillon, W. P., Hoskins, H. and Stephen, R. A. (2003) “Seismic anisotropy in gas-hydrate and gas-bearing sediments on the Blake Ridge, from a walkaway vertical seismic profile,” Geophys. Res. Lett., 30, 1733.

Pecher, I. A., Holbrook, W. S., Stephen, R. A., Hoskins, H., Lizarralde, D., Hutchinson, D. R. and Wood, W. T. (1997) “Offset-vertical seismic profiling for marine gas hydrate exploration - is it a suitable technique? First results from ODP Leg 164,” Proc. 29th Offshore Technology Conference, 193-200.

Pecher, I.A., Milkereit, B., Sakai, A., Sen, M.K., Bans, N.L. and Huang, J.-W. (2010) “Vertical Seismic Profiles through gas-hydrate-bearing sediments,” in: Riedel, Willoughby, Chopra (eds.) Geophysical Characterization of Gas Hydrates, 121-142, Society of Exploration Geophysicists, http://dx.doi.org/10.1190/1.9781560802197.ch8

Pecher, I.A., Minshull, T.A., Singh, S.C. and Huene, R.V. (1996) “Velocity structure of a bottom simulating reflector offshore Peru: Results from full waveform inversion,” Earth and Planetary Science Letters, 139(3–4): 459-469.

Peled, Y., Motil, A., Yaron, L. and Tur, M. (2011) “Slope-assisted fast distributed sensing in optical fibers with arbitrary Brillouin profile,” Optics Express, 19, 19845-19854.

Peled, Y., Yaron, L., Motil, A., Tur, M. (2013 “Distributed and dynamic monitoring of 4km/sec waves using a Brillouin fiber optic-strain sensor,” Fifth Eur. Work Opt. Fibre Sensors. 879434879434.

Perry, K. (2006) "Coiled Tubing Drilling – Cost effective access for CO2 sequestration,” Regional Carbon Sequestration Partnerships Review Meeting. Pittsburg, PA, USA.

Petersen, C.J., Bünz, S., Hustoft, S., Mienert, J. and Klaeschen, D. (2010) “High-resolution P-Cable 3D seismic imaging of gas chimney structures in gas hydrated sediments of an Arctic sediment drift,” Marine and Petroleum Geology, 27(9): 1981-1994.

Pinero, E., Hensen, C., Haeckel, M., Rottke, W., Fuchs, T., and Wallmann, K. (2016) “3-D numerical modelling of methane hydrate accumulations using PetroMod,” Marine and Petroleum Geology 71: 288–295.

Pinkert, S. and Grozic, J. L. H. (2014) “Prediction of the mechanical response of hydrate-bearing sands,” Journal of Geophysical Research: Solid Earth, 119(6), 4695–4707.

Plancke, S. and Berndt, C. (2002) “Anordning for seismikkmåling,” Norwegian Patent no. 317652 (UK Pat. No. GB 2401684; US Pat No. US7,221,620 B2)

Plaza-Faverola, A., Pecher, I., Crutchley, G., Barnes, P.M., Bünz, S., Golding, T., Klaeschen, D., Papenberg, C. and Bialas, J. (2014) “Submarine gas seepage in a mixed contractional and shear deformation regime: Cases from the Hikurangi oblique-subduction margin,” Geochemistry, Geophysics, Geosystems: 15(2): 416-433.

Priest, J. A., Best, A. I. and Clayton, C. R. I. (2005) “A laboratory investigation into the seismic velocities of methane gas hydrate-bearing sand,” J. Geophys. Res., 110, B04102.

Priest, J.A., Best, A.I. and Clayton, C.R.I. (2009) “Influence of gas hydrate morphology on the seismic velocities of sands,” J. Geophys. Res., 114: B11205.

Priest, J.A., Druce, M., Roberts, J., Schultheiss, P., Nakatsuka, Y., Suzuki, K., (2015) “PCATS Triaxial: A new geotechnical apparatus for characterizing pressure cores from the Nankai Trough, Japan,” Mar. Pet. Geol. 66: 460-470.

Riedel, M., Collett, T.S., Malone, M.J., and the Expedition 311 Scientists (2006) Proc. IODP v 311. Available online: http://iodp.tamu.edu/publications/exp311/311title.htm, International Ocean Drilling Program, Texas AM University, College Station TX.

Roscoe, K. H., Schofield, A. N. and Wroth, C. P. (1958) “On the yielding of soils,” Geotechnique, 8(1), 22-53.

Rowe, P.W. (1962) “The stress-dilatancy relation for static equilibrium of an assembly of particles in contact,” Proc. Roy. Soc., 267: 500-527.

Ruppel, C., Boswell, R. and Jones, E. (2008) “Scientific results from Gulf of Mexico Gas Hydrates Joint Industry Project Leg 1 drilling: introduction and overview,” J. Mar. Petrol. Geol., Vol. 25 (9) 819 – 829.

Rutqvist, J., and Moridis, G. J. (2008) “Coupled Hydrologic, Thermal and Geomechanical Analysis of Well Bore Stability in Hydrate-Bearing Sediments,” In Offshore Technology Conference. Offshore Technology Conference.

Ryu, B.-J., Collett, T.S., Riedel, M., Kim, G.-Y., Chun, J.-H., Bahk, J.-J., Lee, J.-Y., Kim, J.-H. and D.-G. Yoo (2013) “Scientific Results of the Second Gas Hydrate Drilling Expedition in the Ulleung Basin (UBGH2),” Marine and Petroleum Geology, 47: 1-20.

Sakai, A. (1999) “Velocity analysis of vertical seismic profile (VSP) survey at JAPEX/JNOC/GSC Mallik 2L-38 gas hydrate research well, and related problems for estimating gas hydrate concentration,” Geol. Survey Can. Bull., 544: 323-340.

Schneider von Deimling, J. and Papenberg, C. (2012) “Detection of gas bubble leakage via correlation of water column multibeam images,” Ocean Sci. Discuss., 8(4): 1757-1775.

Schultheiss, P., Holland, M., Roberts, J., Huggett, Q., Druce, M. and Fox, P. (2011) “PCATS: pressure core analysis and transfer system,” 7th International Conference on Gas Hydrates (ICGH 2011), Edinburgh, Scotland, United Kingdom, July 17-21, 2011.

Schwalenberg, K., E. C. Willoughby, R. Mir, and R. N. Edwards (2005) “Marine gas hydrate electromagnetic signatures in Cascadia and their correlation with seismic blank zones,” First Break, 23: 57–63.

Schwalenberg, K., M. Haeckel, J. Poort, and M. Jegen (2010a) “Evaluation of gas hydrate deposits in an active seep area using marine controlled source electromagnetics: Results from Opouawe Bank, Hikurangi Margin, New Zealand,” Marine Geology, 272 (1-4), 79 - 88.

Schwalenberg, K., W. T. Wood, I. A. Pecher, L. J. Hamdan, S. A. Henrys, M. D. Jegen, and R. B. Coffin (2010b) “Preliminary interpretation of electromagnetic, heat flow, seismic, and geochemical data for gas hydrate distribution across the Porangahau Ridge, New Zealand,” Marine Geology, 272: 89–98.

Schwalenberg, K., Rippe, D., Gehrmann, R., Hoelz, S. (2016) “Marine CSEM Site Survey on Gas Hydrate Targets in the Danube Delta, western Black Sea,” Protokoll über das 26. Schmucker-Weidelt-Kolloquium für Elektromagnetische Tiefenforschung: Dassel 21.-25. September 2015, 26. Schmucker-Weidelt-Kolloquium für Elektromagnetische Tiefenforschung (Dassel 2015), pp. 128—13

Schwalenberg, K., Rippe, D., Koch, S. and Scholl, C. (2017) “Marine-controlled source electromagnetic study of methane seeps and gas hydrates at Opouawe Bank, Hikurangi Margin, New Zealand,” J. Geophys. Res. Solid Earth, 122, doi:10.1002/2016JB013702.

Shankar, U., and Riedel, M., (2011) “Gas hydrate saturation in the Krishna-Godavari basin from P-wave velocity and electrical resistivity logs,” J. of Mar Petr. Geol., 28(10): 1768-1778.

Shen, J., Chiu, C. F., Ng, C. W. W., Lei, G. H. and Xu, J. (2016) “A state-dependent critical state model for methane hydrate-bearing sand,” Computers and Geotechnics, 75: 1-11.

Shengxiong, Y., Jinqiang, L., Yong, L., Yuehua, G., Huaning, X., Hongbin, W., Jingan, L., Holland , M., Schultheiss, P., Jiangong, W., and the GMGS4 Science Team (2017) “GMGS4 Gas hydrate drilling expedition in the South China Sea,” Fire in the ice, 17(1): 7-11.

Spagnoli, G., Finkenzeller, S., Freudenthal, T., Hoekstra, T., Woollard, M., Storteboom, O. and Weixler, L. (2051) “First Deployment of the Underwater Drill Rig MeBo200 in the North Sea and its Applications for the Geotechnical Exploration,” In: Society of Petroleum Engineers (Hrsg.), Proceedings of the SPE Offshore Europe Conference and Exhibition 2015.

Tak, H., Byun, J., Seol, S.J. and Yoo, D.G. (2013) “Zero-offset vertical seismic profiling survey and estimation of gas hydrate concentration from borehole data from the Ulleung Basin, Korea,” J. Marine Pet. Geol. 47: 204-213.

Talukder, A.R. (2012) “Review of submarine cold seep plumbing systems: leakage to seepage and venting,” Terra Nova: 24(4):255-272.

Talukder, A.R., Bialas, J., Klaeschen, D., Buerk, D., Brueckmann, W., Reston, T. and Breitzke, M. (2007) “High-resolution, deep tow, multichannel seismic and sidescan sonar survey of the submarine mounds and associated BSR off Nicaragua pacific margin,” Marine Geology, 241(1-4): 33-43.

Tohidi, B., Anderson, R., Clennell, M. B., Burgass, R. W. and Biderkab, A. B. (2001) “Visual observation of gas-hydrate formation and dissociation in synthetic porous media by means of glass micromodels,” Geology, 29: 867–870

Tinivella, U. and Accaino, F. (2000) “Compressional velocity structure and Poisson's ratio in marine sediments with gas hydrate and free gas by inversion of reflected and refracted seismic data (South Shetland Islands, Antarctica),” Marine Geology, 164(1–2): 13-27.

Tréhu, A., Bohrmann, et al. (2003) Proc. ODP, Init. Repts. 204 [CD-ROM]. Available from: Ocean Drilling Program, Texas A&M University, College Station, TX 11845-9547.

Tréhu, A.M., Bohrman, G., Rack, F.R., Collett, T.S., Goldberg, D.S., Long, P.E., Milkov, A.V., Riedel, M., Schultheiss, P., Tores, M.E., Bangs, N.L., Barr, S.R., Borowski, W.S., Claypool, G.E., Delwiche, M.E., Dickens, G.R., Gracia, E., Guerin, G., Holland, M., Johnson, J.E., Lee, Y.-J., Liu, C.-S., SU, X., Teichert, B., Tomaru, H., Vanneste, M., Watanabe, M. and Weinberger, J.L. (2004) “Three-dimensional distribution of gas hydrate beneath southern Hydrate Ridge: constraints from ODP Leg 204,” Earth and Planetary Science Letters 222:845–862.

Tsuji, Y., Namikawa, T., Fujii, T., Hayashi, M., Kitamura, R., Nakamizu, M., Ohbi, K., Saeki, T., Yamamoto, K., Inamori, T., Oikawa, N., Shimizu, S., Kawasaki, M., Nagakubo, S., Matsushima, J., Ochiai, K. and Okui, T. (2009) “Methane-hydrate occurrence and distribution in the eastern Nankai Trough, Japan: Findings of the Tokai-oki to Kumano-nada methane-hydrate drilling program,” in T. Collett, A. Johnson, C. Knapp, and R. Boswell, eds., Natural gas hydrates—Energy resource potential and associated geologic hazards: AAPG Memoir 89, p. 228–246.

Uchida, S., Deusner, C., Klar, A. and Haeckel, M. (2016) “Thermo-hydro-chemo-mechanical formulation for CH_4-CO_2 hydrate conversion based on hydrate formation and dissociation in hydrate-bearing sediments,” Geo-Chicago 2016 ASCE GSP 270, 235-244.

Uchida, S., Klar, A. and Yamamoto, K. (2016) “Sand production model in gas hydrate-bearing sediments,” International Journal of Rock Mechanics and Mining Sciences, 86: 303–316.

Uchida, S., Levenberg, E., and Klar, A. (2015) "On-specimen strain measurement with fiber optic distributed sensing," Measurement, 60: 104–113.

Uchida, S., Xie, X.-G. and Leung, Y.F. (2016) “Role of critical state framework in understanding geomechanical behavior of methane hydrate-bearing sediments,” Journal of Geophysical Research 121(8), 5580-5595.

Uchida, S., Soga, K. and Yamamoto, K. (2012) "Critical state soil constitutive model for methane hydrate soil," Journal of Geophysical Research: Solid Earth, 117(B3), 1-13.

Virieux, J. and Operto, S. (2009) “An overview of full-waveform inversion in exploration geophysics,” Geophysics, 74(6): WCC1-WCC26.

Walia, R., Mi, Y., Hyndman, R. D. and Sakai, A. (1999) “Vertical seismic profile (VSP) in the JAPEX/JNOC/GSC Mallik 2L-38 gas hydrate research well, In Scientific Results from JAPEX/JNOC/GSC Mallik 2L-38 Gas Hydrate Research Well, Mackenzie Delta, Northwest Territories, Canada,” (ed.) S.R. Dallimore, T. Uchida, and T.S. Collett; Geological Survey of Canada, Bulletin, 544: 341-355.

Wallmann, K. and Bialas, J.R. (2009) “SUGAR (submarine gas hydrate reservoirs)”, Environmental Earth Sciences, 59(2): 485-487.

Wallmann, K., Pinero, E., Burwicz, E., Haeckel, M., Hensen, C., Dale, A. and Ruepke, L. (2012) “The Global Inventory of Methane Hydrate in Marine Sediments: A Theoretical Approach,” Energies, 5(12): 2449-2498.

Wang, X., Qian, R. and Xia, C. (2014) “PS-wave processing and S-wave velocity inversion of OBS data from Northern South China Sea,” Journal of Applied Geophysics, 100: 58-65.

Weitemeyer, K. A., Constable, S. C., Key, K. W. and Behrens, J. P. (2006) “First results from a marine controlled-source electromagnetic survey to detect gas hydrates offshore Oregon,” Geophys. Res. Let. 33. doi:10.1029/2005GL024896.

Weitemeyer, K. A., Constable, S. and Trehu, A. M. (2011) “A marine electromagnetic survey to detect gas hydrate at Hydrate Ridge, Oregon,” Geophys. J. Int, doi: 10.1111/j.1365-246X.2011.05105.x.

Weitemeyer, K. and Constable, S. (2010) “Mapping shallow geology and gas hydrate with marine CSEM surveys,” First Break, 28, 97-102

Westbrook, G.K., Carson, B., Musgrave, R.J. et al. (1994) Proc. ODP, Init. Repts, 146, College Station, TX (Ocean Drilling Program).

White, M. D., and Oostrom, M. (2006) “STOMP Subsurface Transport Over Multiple Phase: User’s Guide,” Pacific Northwest National Laboratory, Washington.

Winters, W. J., Waite, W. F., Mason, D. H., Gilbert, L. Y. and Pecher, I. A. (2007) “Methane gas hydrate effect on sediment acoustic and strength properties,” Journal of Petroleum Science and Engineering 56(1): 127–135.

Yamamoto, K. (2016) “Overview and introduction: Pressure core-sampling and analyses in the 2012-2013 MH21 offshore test of gas production from methane hydrates in the eastern Nankai Trough,” Marine and Petroleum Geology, 66: 296–309.

Yamamoto, K. and Ruppel, C., (2015) “Preface to the special issue on gas hydrate drilling in the Eastern Nankai Trough,” J. Mar. Petr. Geol., 66(2): 295

Yamamoto, K., Terao, Y., Fujii, T., Ikawa, T., Seki, M., Matsuzawa, M. and Kanno, T. (2014) “Operational overview of the first offshore production test of methane hydrates in the Eastern Nanaki Trough,” Offshore Technology Conference, 05-08 May, Houston, Texas, OTC-25243-MS.

Yuan, J. and Edwards, R. N. (2000) “The assessment of marine gas hydrates through electrical remote sounding: hydrate without a BSR?,” Geophys. Res. Let. 27: 2397–2400.

Yu, H.S. (1998) “CASM: a unified state parameter model for clay and sand,” International Journal for Numerical and Analytical Methods in Geomechanics, 22(8):621–653.

Yun, T.S., Francisca, F.M., Santamarina, J.C. and Ruppel, C. (2005) “Compressional and shear wave velocities in uncemented sediment containing gas hydrate,” Geophysical Research Letters, 32(10): 10.1029/2005GL022607.

Yun, T. S., Santamarina, J. C. and Ruppel, C. (2007) “Mechanical properties of sand, silt, and clay containing tetrahydrofuran hydrate,” J. Geophys. Res. 112(B4): 1–13.

Zadok, A., Antman, Y., Primerov, N., Denisov, A., Sancho, J. and Thevenaz, L. (2012) "Random-access distributed fiber sensing," Laser & Photon. Rev., 6: L1–L5.

Zander, T., Haeckel, M., Berndt, C., Chi, W.-C., Klaucke, I., Bialas, J., Klaeschen, D., Koch, S. and Atgın, O. (2017) “On the origin of multiple BSRs in the Danube deep-sea fan, Black Sea,” Earth and Planetary Science Letters, 462: 15-25.

Zillmer, M., Flueh, E.R. and Petersen, J. (2005) “Seismic investigation of a bottom simulating reflector and quantification of gas hydrate in the Black Sea” Geophysical Journal International, 161(3): 662-678.